Bernardo Fitas Sarmento

Bachelor of Science in Materials Engineering

Simulation of sunlight driven CO_2 conversion to CH_4 to satisfy a single-house heating requirements

Dissertation submitted in partial fulfillment
of the requirements for the degree of

Master of Science in
Materials Engineering

Supervisor: Dr. Ana Reis Machado, Auxiliar Researcher, NOVA University of Lisbon

Co-supervisors: Dr. Manuel J. Mendes, Post-Doc Fellow and Invited Assistant Professor, NOVA University of Lisbon

Dr. Jorge Manuel Facão, Researcher, Laboratório Nacional de Energia e Geologia

Examination Committee

Chairperson: Dr. João Paulo Borges, NOVA University of Lisbon
Raporteur: Dr. Maria João de Carvalho, Laboratório Nacional de Energia e Geologia
Member: Dr. Ana Reis Machado, NOVA University of Lisbon

FACULDADE DE
CIÊNCIAS E TECNOLOGIA
UNIVERSIDADE NOVA DE LISBOA

October, 2018

Simulation of sunlight driven CO_2 conversion to CH_4 to satisfy a single-house heating requirements

This document was created using the (pdf)LaTeX processor, based in the "novathesis" template[1], developed at the Dep. Informática of FCT-NOVA [2].
[1] https://github.com/joaomlourenco/novathesis [2] http://www.di.fct.unl.pt

Acknowledgements

Quero começar por agradecer ao Professor Doutor Rodrigo Martins como presidente do Departamento de Ciências dos Materiais e à Professora Doutora Elvira Fortunato como directora do Centro de Investigação de Materiais por todo o apoio e dedicação em tornar o DCM e o CENIMAT em centros de ensino e de investigação de topo e por proporcionarem aos alunos as mais altas condições de ensino.

Obrigado aos meus orientadores, Profª. Doutora Ana Machado, Prof. Doutor Manuel Mendes e Doutor Jorge Facão pela oportunidade de poder participar num projecto tão interessante para a sociedade e por toda a ajuda, paciência e apoio dado no decorrer do meu trabalho.

Quero agradecer também ao DCM e a todos os professores que me abilitaram com as ferramentas necessárias que me tornaram num engenheiro e numa melhor pessoa e que continuem com o excelente trabalho de formar futuros Engenheiros de Materiais.

Um muito obrigado às pessoas que me acompanharam durante estes 5 anos, pelas horas de estudo em conjunto, pelas noitadas a fazer trabalhos por chamada, pelas brincadeiras, pelos sorrisos, pelas idas ao sushi, por estarem sempre lá e pelas amizades criadas para a vida toda.

Finalmente um agradecimento à minha família e muito especial à minha Mãe, Pai e Irmão, obrigado por me darem a educação e a possibilidade de frequentar a faculdade e por todo o apoio e amor incondicional.

Obrigado a todos!

If we are to live,
We must take risks.
Else our lives become
Deaths in all but name.
There is no struggle too vast,
No odds too overwhelming,
For should we fail - should we fall -
We will know
That we have
Lived.

Steven Erikson

Abstract

The rise of Earth's atmospheric CO_2 levels, primarily due to combustion of fossil fuels, has affected its ecosystems. A way to combat this is by mimicking the plants photosynthesis by capturing CO_2 from the atmosphere and convert it to usable hydrocarbon fuels, such as methane (CH_4), because of the easy adaptability to the well-established infrastructure for natural gas (NG) storage, distribution and consumption. The denominated "solar methane", very similar to NG, can be produced by converting solar energy from photovoltaic (PV) panels into electricity to power a 1-step reaction on electrochemical flow cell(s), using CO_2 and water as the feedstock. Here, we simulate solar methane production and storage and apply it to address the energetic needs of concept buildings that have space and domestic hot water heating requirements. A combination of solar thermal collectors (STCs) and PV panels is optimized for buildings in different European locations, in which the heating needs that cannot be fulfilled by the STCs are satisfied by the combustion of methane synthesized by the PV-powered electrolyzers. Various combinations of situations for a whole year were studied and it was found that this auxiliary system can produce, per m^2 of PV area, in the worst case scenario 23.6 g/day (0.328 kWh/day) of methane in Stockholm and in the best case scenario 47.4 g/day (0.658 kWh/day) in Lisbon.

Keywords: Systems Simulations, Artificial Photosynthesis, Photovoltaic-Electrochemical CH_4 production, Methanation, Building Integrated Solar Fuels, TRNSYS modelling

Resumo

O aumento dos níveis de CO_2 na atmosfera terrestre, principalmente devido à combustão de combustíveis fósseis, tem afectado os ecossistemas. Uma maneira de combater isto é imitando o processo de fotossíntese das plantas ao capturar CO_2 da atmosfera e converter em combustíveis hidrocarbonetos utilizáveis, tal como o Metano (CH_4), devido à fácil adaptabilidade à infraestructura já estabelecida de gás natural (NG) para armazenamento, distribuição e consumo. O denominado "metano solar", muito idêntico ao NG, pode ser produzido convertendo energia solar de painéis fotovoltaicos (PV) em eletricidade para promover numa célula electroquímica a conversão de CO_2 e água em metano num só passo. Neste trabalho, simulamos a produção de metano solar e o seu armazenamento para satisfazer as necessidades energéticas de edifícios de conceito com requerimentos de aquecimento ambiente e de preparação de água quente sanitária. Uma combinação de colectores solares térmicos (STC) e paineis PV são otimizados para edifícios em diferentes cidades Europeias. Caso as necessidades energéticas não possam ser satisfeitas pelos STCs, são satisfeitas pela combustão do metano sintetizado. Várias combinações de situações para um ano inteiro foram estudadas e descobriu-se que este sistema auxiliar pode produzir, por m^2 de PV area, no pior cenário 23.6 g/dia (0.328 kWh/dia) de metano em Estocolmo e no melhor cenário 47.4 g/dia (0.658 kWh/dia) em Lisboa.

Palavras-chave: Simulação de sistemas, Photossíntese artificial, Metanação, Edifício integrado com combustíveis solares, Fotovoltaico-Electroquímica produção de CH_4, modelação em TRNSYS

Contents

List of Figures

List of Tables

Listings

Glossary

Energy content of hot water	(Q_{tap}) Means the product of the specific heat capacity of water, the average temperature difference between the hot water output and cold water input, and the total mass of the hot water delivered [1].
g-Value	The g-value is a measure of how much solar heat (infrared radiation) is allowed in through a particular part of a building. A low g-value indicates that a window lets through a low percentage of the solar heat.
Load profile	Means a given sequence of water draw-off [1].
Passive house	A passive house is a building standard that is truly energy efficient, comfortable, affordable and ecological at the same time. They require less than 15 kWh/m^2.year for space heating [2].
Peak temperature	(T_p) Means the minimum water temperature, expressed in degrees Celsius, to be achieved during water draw-off [1].
Useful energy content	(Q_{tap}) Means the energy content of hot water, expressed in kWh, provided at a temperature equal to, or above, the useful water temperature, and at water flow rates equal to, or above, the useful water flow rate [1].
Useful water temperature	(Tm) Means the water temperature, expressed in degrees Celsius, at which hot water starts contributing to the reference energy [1].
Useful water flow rate	(f) Means the minimum flow rate, expressed in litres per minute, for which hot water is contributing to the reference energy [1].
u-Value	The u-value is a measure of how much heat escapes via the windows, walls and roof for example. The U-value is often measured for the whole window structure with the combination of glass, frame and sash. The lower the U-value, the better the insulating capacity of the window.

Water draw-off — Means a given combination of useful water flow rate, useful water temperature, useful energy content and peak temperature [1].

Acronyms

η	Faradaic efficiency (electricity-to-fuel).
θ	Incidence Angle on Solar Thermal Collectors.
η_{STC}	Solar Thermal Collector efficiency.
A	Diode factor.
a_0	Intercept (maximum) of the collector efficiency.
a_1	Negative of the first-order coefficient in collector efficiency equation.
a_2	Negative of the second-order coefficient in collector efficiency equation.
b_0	Parameter in 2nd degree polynomial equation for IAM modifying factor..
b_1	Parameter in 2nd degree polynomial equation for IAM modifying factor..
CCU	Carbon Capture and Utilization.
CSTB	Scientific and Tecnical Centre for Building.
DAC	Direct Air Capture.
DHW	Domestic Hot Water.
EC	Electrochemical Cell.
EC-IV	Electrochemical Cell - Current vs Voltage curve.
FF	Fill Factor.
HE	Heat Exchanger.
I_{MPP}	Current at maximum point.
I_{PH}	Photocurrent.
I_{SAT}	Reverse Saturation Current.
I_{SC}	Short Circuit Current.
I_T	Global radiation incident on the solar collector (Tilted surface).

IAM	Incidence Angle Modifier.
LNEG	Laboratório Nacional de Energia e Geologia.
MATLAB	MATrix LABoratory.
P_{MPP}	Power at Maximum Point.
PV	Photovoltaic.
PV-IV	Photovoltaic panel - Current vs Voltage curve.
q	Elementary charge.
Q_{AuxHE}	Energy supplied by the auxiliary electric resistance in the Heat Exchanger.
Q_{AuxT}	Energy supplied by the auxiliary electric resistance in the Tank.
Q_{DHW}	Energy demanded for Domestic Hot Water.
Q_{SH}	Energy demanded for Space Heating.
Q_{STC}	Energy supplied by the Solar Thermal Collectors.
Q_{TL}	Energy lost in the tank by thermal losses.
R_S	Series Resistance.
R_{SH}	Shunt Resistance.
SH	Space Heating.
SNG	Synthetic Natural Gas or Substitute Natural Gas.
STC	Solar Thermal Collector.
T	Temperature.
T_{amb}	Ambient Temperature.
TC	Cell temperature.
TESS	Thermal Energy Systems Specialists.
TRNSYS	TRaNsient SYstem Simulation.
V_{MPP}	Voltage at maximum point.
V_{OC}	Open Circuit Voltage.

Chapter 1

Objectives and Motivation

The energy crisis and global warming have become a serious issue and every year the annual global CO_2 emissions increase and fossil fuel emissions account for about 91% of total carbon dioxide emissions from human sources in 2014[3]. Solar Driven CO_2 reduction has attracted more and more attention as the key technology to ensure a stable supply of energy as renewable alternative to fossil fuels. Using methane as the end product of such system is very advantageous because of the already well-established infrastructure for natural gas storage, distribution and consumption. The author takes also the responsibility to contribute to the transition to renewable energies sources otherwise future generations may not survive.

With this work we aim to understand how a solar methane generation system could be implemented in a single family house concept building to satisfy space heating and domestic hot water heating requirements in different locations with different solar thermal collectors, PV panels and EC configurations.

Chapter 2

Introduction

2.1 Solar Fuels Generation

Carbon dioxide is a major greenhouse gas resulting from human activities. In the past centuries, utilization of carbon-rich fossil fuels - coal, oil and natural gas - has allowed an unprecedented era of prosperity and advancement for human development but also the increase of its concentration in the atmosphere from ~278 ppm before the industrial revolution to 403 ppm in 2016[1]. The increase in CO_2 emissions arguably contributes to the increase in global temperature and climate change due to the greenhouse effect [4], posing a critical threat to the environment. Also, because of the highly dependence of fossil fuels for energy production worldwide and despite their considerable size, fossil fuels reserves are finite, limited and will, therefore, be increasingly depleted. A novel approach that is attracting a significant amount of interest is carbon capture and utilization (CCU), whereby captured CO_2 is converted into a diversity of chemical products including liquid hydrocarbons. The fuels produced via this route would replace an equivalent amount of fossil fuels, creating an almost closed loop of sustainable fuels utilization [5].

Because of solar energy intermittence, solar fuels generation is an attractive option with the advantage of capturing much of the photon energy in the bonds of portable and energy dense chemical species such as hydrogen or liquid hydrocarbons. This process can be achieved through the carbon-free hydrogen synthesis via water splitting and by electrolysis, thermochemical decomposition, photoelectrochemical dissociation via the carbon–neutral combination of water-splitting with electrochemical CO_2 reduction reaction (CO_2RR) to hydrocarbons fuels.

We will simulate methane generation in a flow electrochemical cell of water electrolysis with electrochemical CO2RR, figure 2.1, because of the direct 1-step fuels generation (equation 2.2). Ideally, the reduction should yield to a single energy-rich compound. However, selective methane production remains a challenging task at present due to multiple proton-coupled electron transfer steps involved in the reaction [6]. Despite the fact that this approach is still in the lab stage, it has been shown that methane could be obtained with high selectivity. The simulation is based on the work of *Manthiram et al* [7] on enhancing the eletrochemical methanation of carbon dioxide in 1-step with a dispersible

[1] according to WMO Greenhouse bulletin No. 13 in 30 October 2017

nanoscale copper catalyst.

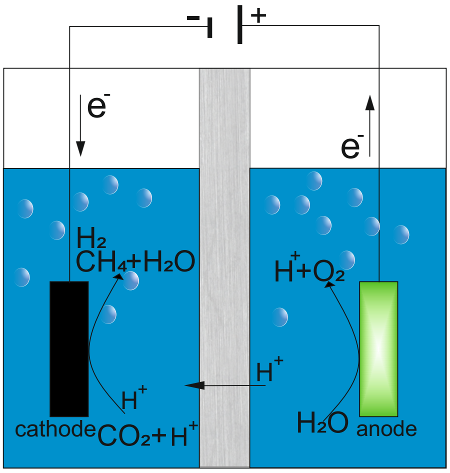

Figure 2.1: Scheme of the Electrochemical cell with the 1-step methane production

Another limitation of this process is the hydrogen competitive generation (eq. 2.1) with CO_2 reduction (eq. 2.2), due to both reactions [8] having similar thermodynamic potential — 1.23 V for water splitting and 1.06 V for CO_2 reduction — consequently, we have low faradaic efficiency for CH_4 generation.

$$2H_2O \xrightarrow{e^-} 2H_2 \uparrow + O_2 \uparrow \qquad \Delta G^o = 474.33 kJ/mol \tag{2.1}$$

$$CO_2 + 2H_2O \xrightarrow{e^-} CH_4 \uparrow + 2O_2 \uparrow \qquad \Delta G^o = 818.18 kJ/mol \tag{2.2}$$

Various authors have noticed that the deactivation of copper electrodes occurs [9] after a few hours producing CH_4. In this simulation work, we will consider that the EC has stable performance throughout the year. However, to have an idea how electrode deactivation can affect solar methane production a lower faradaic efficiency was also considered. Thus, for voltage > 2.9V, the last value on the experimental data for CH_4 faradaic efficiency from *Manthiram et al.*, we will consider 60% and 40% efficiency for, respectively, good electrode performance and deactivation performance.

Although the low concentration of CO_2 in air for direct air capture (DAC) requires the treatment of high volumes, it has been investigated since half a century and has been applied in cryogenic oxygen separation plants [10]. DAC may use solid sorbents or aqueous basic solutions as capture media. Solid sorbents offer the possibility of low energy input, low operating costs and applicability across a wide range of scales but with the challenges that a very large structure has to be built at low cost while allowing the structure to be periodically sealed from the ambient air during the regeneration step and the conflicting demands of high sorbent performance, low cost and long economic life in impure ambient air. Aqueous sorbents offer the advantage that the contactor can operate continuously, can be built using cheap cooling-tower hardware and allows very long contactor lifetimes despite dust and atmospheric contaminants. Disadvantages include the cost and complexity of the regeneration system and water loss in dry environments [11].

2.1.1 Integrated Photovoltaic-Electrochemical CO_2 Reduction

Some authors investigated the design and modulation of an off the grid photovoltaic (PV) system for hydrogen production using methanol electrolysis achieving 24.38 $g/m^2{}_{PV}$ per day with PV array on a tilted surface [12]. It was reported in 2015 by *Grätzel* [13] workgroup a device driven solely by sunlight using water as electron source to reduce CO_2 to carbon monoxide. They achieved a solar-to-CO efficiency of 6.5%. *Meenesh R. Singh et al* [14] team showed in 2015 that solar-to-methane efficiencies for photovoltaic electrolyzers can operate at 7.2% with a thermodynamic limit at 41.8%, meaning that there is considerable opportunity for further improvement.

Some authors also analyzed methane production by PV panels, an electrolyser and Sabatier reactor and CO_2/CH_4 conversion rate of 81% was obtained [15] and others optimized the Solargas process with different operating parameters [16]. However, this requires a Sabatier reactor and high pressure gases to achieve greater yield. *Jordi Guilera et al.* produced an article related to the economic viability of synthetic natural gas (SNG) production from power, carbon dioxide and oxygen to methane and concluded that the state of the art tecnology at the moment can produce SNG 2-7 times higher than conventional natural gas but this value could reduce up to 40 EUR/MWh, really close to the current price of conventional gas[17].

2.2 Building Heating Requirements

In 2016, the households or residential sector represented 25.4% of final energy consumption in the EU. Households use energy for various purposes: space and water heating, space cooling, cooking, lighting and electrical appliances. According to Eurostat [18], the EU-28 final energy consumption in the residential sector in 2016 for natural gas (NG) was 36.9%. In the residential sector, natural Gas plays an essential role in terms of space heating, water heating and cooking with, respectively, 43.4%, 47.9% and 33.1% of energy consumed for these end-uses (fig. 2.2). NG composition varies among different regions and suppliers but, generally, it consists 93.9% of methane [19], a compound with one carbon atom and four hydrogen atoms, 4.2% ethane, a compound with two carbons atoms and 6 hydrogen atoms, and a minor part of other gases. Because of solar energy's abundance, methane high energy density of 50 MJ/kg [20] and an already existent infrastructure for storage, transport and consumption, producing the so called "solar methane" is one of the most promising approaches to fill the need for energy.

For the building heating needs, we will use the software TRaNsient SYstem Simulation (TRNSYS) and the building assistance guide (TRNBuild) (fig.2.4) to develop a single

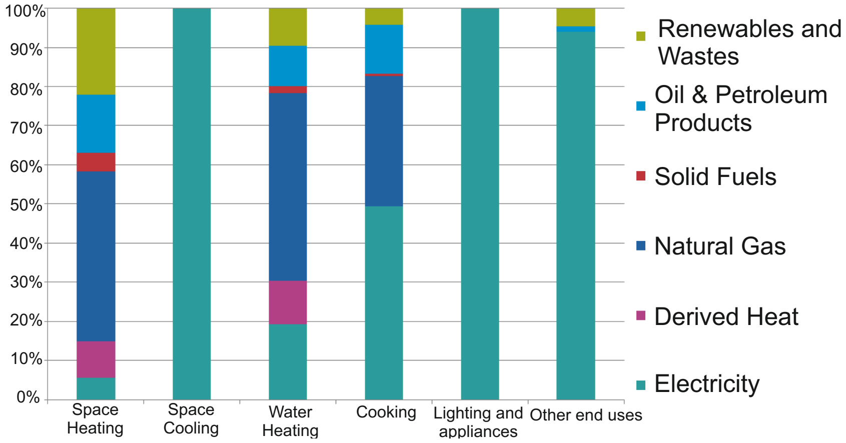

Figure 2.2: Final energy consumption in the residential sector by type of end-uses for the main energy products, EU-28, 2016[18]

family concept building, figure 2.3, with a central heating system connected to a storage tank that provides the necessary heating requirements for Space Heating (SH) and Domestic Hot Water (DHW). It has Solar Thermal Collectors (STCs) to provide part of the heating needs and if the heating needs cannot be fulfilled by the STCs, then they are satisfied by the combustion of stored methane synthesized by the PV-powered electrolyzers. We will use MATLAB software to simulate a conversion system that uses solar energy from PV panels into electricity to power a 1-step reaction in a electrochemical (EC) flow cell(s), using CO_2 and water as feedstock, in an attempt to show the possible viability of such system integrated in future houses.

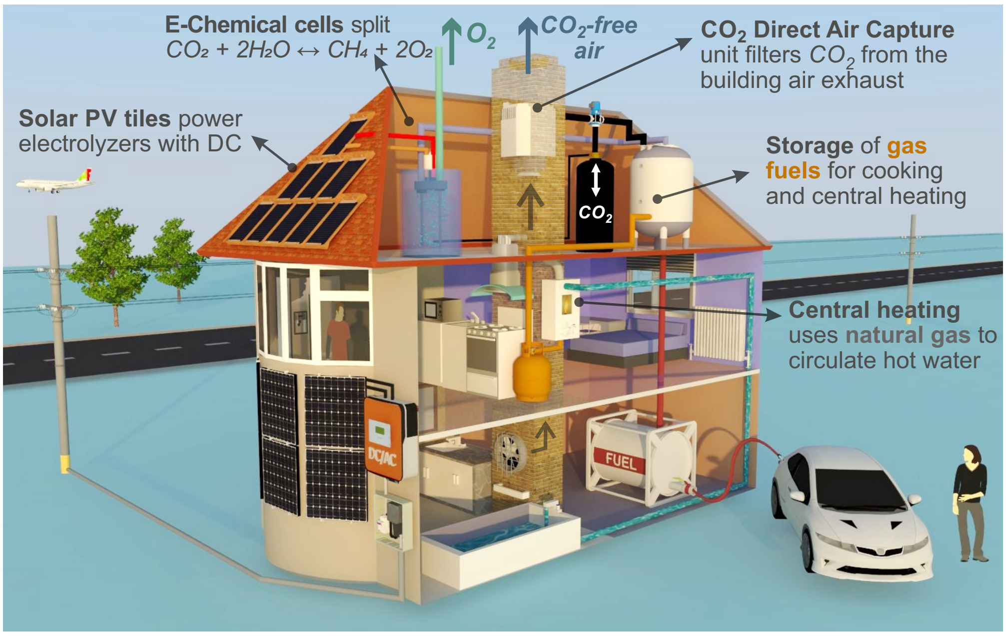

Figure 2.3: Illustration of the concept house. The energy harnessed by PV panels powers the electrolyzers to produce methane that is stored for future use.

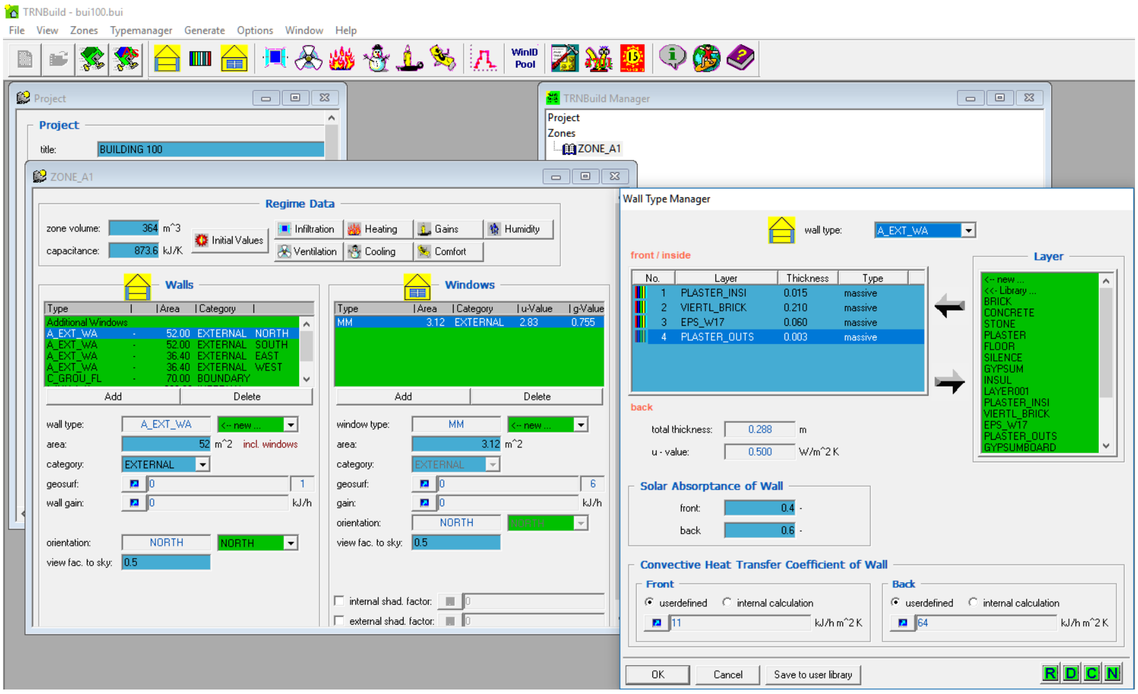

Figure 2.4: TRNBuild Interface

The aim of the present work is to investigate how solar methane can be produced in residential buildings for in house combustion to satisfy heating needs. For this, three locations will be considered: Lisbon in Portugal, Grenoble in France and Stockholm in Sweden. The building walls and windows specifications were built according to the space heating needs for each location. In Lisbon and Grenoble, a passive house with 15 kWh/m^2.year of space heating was studied. In order to test a building less efficient, we also considered one with higher SH energy demand, 100 kWh/m^2.year, only for Grenoble and Stockholm. Another variable under study is STCs area where commercially available STCs were considered and we tested two different areas, 4 and 6 m^2.

This thesis is organised as follows: chapter 3 explains the software and methodology used. Chapter 4 provides a section related to TRNSYS with a full description of the enviornment on TRNSYS and another section on how the core of the Matlab script to produce methane works and afinal section is presented with the results achieved. The last chapter will be directed at the conclusions of the entire work and future perspectives.

Chapter 3

Architecture of the System

3.1 Software used

3.1.1 TRNSYS

TRNSYS is a complete extensible simulation environment for the transient simulation of systems, including multi-zone buildings. It was originally developed by the Solar Energy Laboratory in University of Winsconsin, Madison, USA[**trnsys_ref**] but then it was also developed on continuously partnership with TRANSSOLAR Energietechnik GmbH[1], Thermal Energy Systems Specialists (TESS)[2] and Scientific and Tecnical Centre for Building (CSTB)[3]. The most recent version is 18 released in 2017 but version 16 was used for this work from license number available from Laboratório Nacional de Energia e Geologia (LNEG), Portugal.

TRNSYS is used by engineers and researchers around the world because of its versatility and allows to validate new energy concepts, from simple domestic hot water systems to the design and simulation of buildings and their equipment, including occupant behaviour and alternative energy systems (wind, solar, photovoltaic, hydrogen systems, fuel cells).

TRNSYS consists of a suite of programs: the TRNSYS Simulation Studio, which is the main visual interface, the simulation engine (TRNDll.dll), its executable (TRNExe.exe) and the building input data visual interface (TRNBuild.exe).

A TRNSYS project is typically setup by connecting components graphically in the Simulation Studio, by drag-and-dropping components in the workspace, connecting them together and setting the global simulations parameters. Each component, also called type, is described by a mathematical model in the TRNSYS simulation engine and has a set of matching proforma's in the simulation studio. The proforma has a black-box description of a component: inputs, outputs and parameters that can be personalized for the specific simulation environment [21].

[1] https://transsolar.com/
[2] http://www.tess-inc.com/
[3] http://www.cstb.fr/

3.1.2 MATLAB

MATLAB (*MATrix LABoratory*) is a tool for technical computing, computation and visualization in an integrated environment and is developed by The MathWorks[4]. The license used was from Faculdade de Ciências e Tecnologias da Universidade Nova de Lisboa. Various scripts were created to automatize the processing and analysation of the TRNSYS simulation studio data outputs and the parameters used can be found in the annex I.

3.2 Methodology

The methodology used for this thesis is described in figure 3.1.

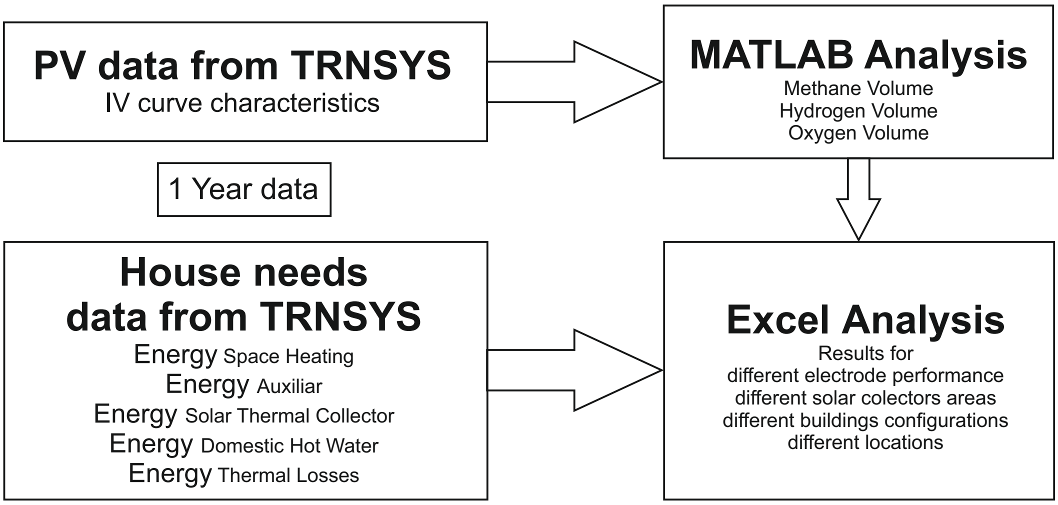

Figure 3.1: Scheme of the methodology used

In order to test this concept, three locations were chosen: Lisbon in Portugal (N 38º 43” W 9º 9”), Grenoble in France (N 45º 22” E 5º 20”) and Stockholm in Sweden (N 59º 21” E 17º 57”). We also tested the house needs for space heating and domestic hot water consumption of two type of homes: a passive house with 15 kWh/m^2.year on space heating (SH) consumption for Lisbon and Grenoble and a more standard house with 100 kWh/m^2.year SH consumption for Grenoble and Stockholm. Because we also wanted to see the influence of different solar thermal collectors areas on our building, we also tested for STCs areas of 4 and 6 m^2. To test the performance of our Electrochemical cell (EC) when considering electrode deactivation for voltage >2.9V, we will consider a faradaic efficiency of 60% and 40%.

[4]https://www.mathworks.com/

Chapter 4

Discussion and results

4.1 TRNSYS Parameters

In this chapter, the building description and the most important TRNSYS files parameters are defined, everything not listed remained as default in the TRNSYS environment. The output values are saved at each instance of the simulation in a text file which are then processed by MATLAB and Excel.

4.1.1 Main Project

Each TRNSYS simulation ran for 8766 hours, simulating 1 year, with a time step of 90 seconds and successive substitution as the solution method. Tolerance integration and convergence errors are both set to 0.001. The main project is represented in fig. 4.1 and is divided in 4 sections: the building itself and its vital connections (red lines), space heating calculation loop (purple lines), the solar collector loop (dark blue lines) and the domestic hot water loop (green lines). The way this simulation works is by every section giving or taking heat from the tank (type60d) which is fed by the solar collector. If any additional heat is needed, the tank activates an electric resistance that provides the auxiliary heat required (Qaux) which is then printed at every timestep to a file. Outside the TRNSYS environment, Qaux is then converted to the equivalent quantity of methane as it was combusted in a boiler with an efficiency of 90%.

In order to store heat in the form of hot water, we simulated the use of tank (type60d) with 2 heat exchangers, one for space heating and another for the solar collector loop and an electric auxiliary heater that kicks in when the STCs are not gathering enough heat to suppress the house heating needs. A second electric auxiliary was exclusively used for space heating requirements. Also, to foresee domestic hot water (DHW) consumption we used eight Time Dependent Forcing Functions, 4 for Water Draw (type14b) and another 4 for water Temperature (type14e), with a water load profile M from European Journal [1] with conjunction with a diverter (type11b) and a tee piece (type11h) to work as a mixing valve for hot and cold water to get the desired temperature for domestic water use.

Finally, to simulate our meteorological conditions, we used the component for Data Reader and Radiation Processor (type109) and the weather files from Meteonorm 7.1 from

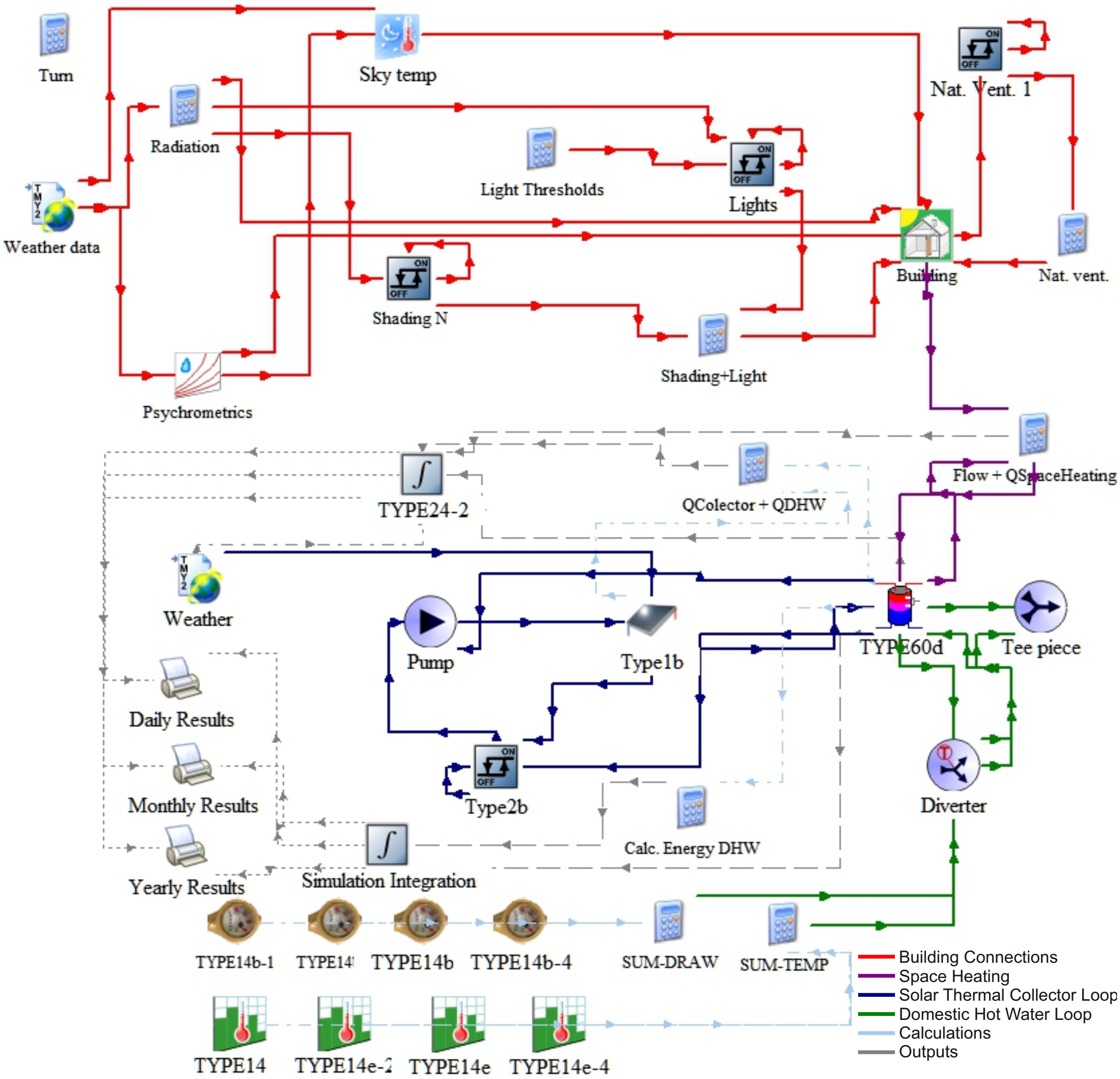

Figure 4.1: Printscreen from TRNSYS Studio environment. Red lines represent the building connections, dark blue lines represent the solar collector loop, green lines represent the DHW loop, light blue lines represent calculations, grey lines represent outputs

METEOTEST [1], the license number was used from LNEG, referring to the radiation data from 1991-2010 and temperature and other parameters from 2000-2009. Three different locations in Europe were used for this work: Lisbon in Portugal, Grenoble in France and Stockholm in Sweden.

For this work, we simplified the combustion of CH_4 system and used the tank's auxiliary heating rate output value to mimic the burning, similar to what a boiler would burn natural gas (94% is methane) to heat water into the tank and a 90% conversion efficiency was considered. The reference building is defined in the following chapter, including architectural design and orientation as well as constructive descriptions of all building elements such as walls, floors, windows and roof.

[1] https://meteotest.ch/

4.1.1.1 Building Parameters

For this work, it was used the building project helping assistance guide for multi-zone buildings from TRNSYS to build our test building in two different conditions: bui15 and bui100 related to a building that consumes 15 kWh/m^2 year and bui100 for 100 kWh/m^2 year, respectively, in space heating. This multi-zone building component model (type56) is a non-geometrical balance model with one air node per zone, representing the thermal capacity of the zone air volume and capacities which are closely connected with the air node (furniture, for example). Thus the node capacity is a separate input in addition to the zone volume [22].

The reference buildings are based on the *Task 32 for project report A2 of subtask A: The Reference Heating System, the template Solar system* made by Solar Heating & Cooling Programme, International Energy Agency (SHC). The building naming references to their heating loads, such as 15 and 100 kWh/m^2.year. Both have the same architectural design but different insulation thickness for distinct locations as described in figure 4.2 and table 4.1.

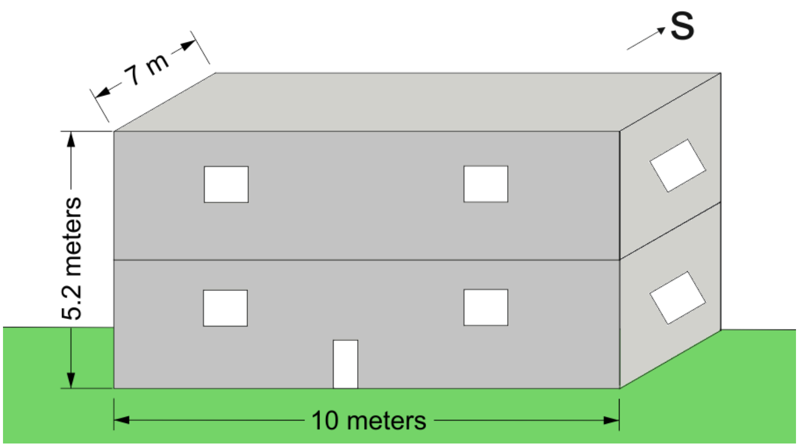

Figure 4.2: Scheme of the building dimensions

The building is a two storey housing, with effective floor area as 70 m^2 per store. The window area on the South, North, West and East façades are, respectively, 25%, 6%, 10% and 10%. Both floors are simulated as one common thermal zone with 200m^2 of internal walls and a total volume area of 364 m^3. The house used in this work was made using TRNSYS multizone building project assistant and was simplified in terms of dimensions and number of zones. The various materials, layer thicknesses and energy performance describing the buildings bui15 and bui100 are listed in Table 4.1.

The building has an airchange infiltration rate of 0.8/h, airchange of ventilation off, humidification off, heating on with unlimited power and cooling was turned off. A simple humidity model with a capacitance ratio 1 was used and the comfort for the zone was also turned off. The window layout materials was used from TRNSYS American lib files and are described in Table 4.2.

Table 4.1: Construction building elements for 15 and 100 kWh/m^2.year houses. L15 is for Lisbon, G15 and G100 is for Grenoble, and S100 is for Stockholm

Assembly	Layer	layer thickness L15 (m)	G15 (m)	G100 (m)	S100 (m)	Conductivity (kJ h^{-1} m^{-1} K^{-1})	Capacity (kJ Kg^{-1} K^{-1})	Density (kg m^{-3})	U-Value construction L15 (W m^{-2} K^{-1})	G15	G100	S100
Ground Floor	Wood	0.015	0.015	0.015	0.015	0.5400	2.50	600	0.173	0.439	0.158	0.225
	Plaster Floor	0.060	0.060	0.060	0.060	5.0400	1.00	2000				
	XPS	0.200	0.070	0.220	0.150	0.1332	1.45	38				
	Concrete	0.150	0.150	0.150	0.150	7.5600	0.80	2400				
Total		0.425	0.295	0.445	0.375							
External Floor	Plaster Inside	0.015	0.015	0.015	0.015	2.1600	1.00	1200	0.178	0.235	0.333	0.228
	Viertl brick	0.300	0.210	0.210	0.300	2.5200	1.00	1380				
	EPS	0.200	0.150	0.100	0.150	0.1440	1.45	17				
	Plaster Outside	0.003	0.003	0.003	0.003	2.5200	1.00	1800				
Total		0.518	0.378	0.328	0.468							
Roof	Gympsumboard	0.025	0.025	0.025	0.025	0.7600	1.00	900	0.207	0.317	0.291	0.291
	Plywood	0.015	0.015	0.150	0.015	0.2916	2.50	300				
	Rockwool	0.150	0.090	0.100	0.100	0.1296	1.03	60				
	Plywood	0.015	0.015	0.150	0.015	0.2916	2.50	300				
Total		0.205	0.145	0.425	0.155							
Internal Wall	Clinker Brick	0.200	0.200	0.200	0.200	0.8280	0.92	650	0.962			

Table 4.2: Thermal properties of windows for the 15 and 100 kWh/m^2.year building

Location	Bui. Heating Load (kWh m^{-2} year^{-1})	Uwindow (W m^{-2} K^{-1})	g-Value	Uframe (kJ h^{-1} m^{-2} K^{-1})	Construction (mm)	Window ID
Lisbon	15	5.74	0.87	8.17	4/16/4/16/4	1001
Grenoble	15	2.83	0.755	8.17	4/16/4	1202
Grenoble	100	5.74	0.87	8.17	4/16/4/16/4	1001
Stockholm	100	2.83	0.755	8.17	4/16/4	1202

4.1.1.2 Storage Tank

The type 60d is used to simulate the storage tank and a scheme can be found in figure 4.3. Two heat exchangers (HE) are used to simulate the solar collector heat input and the heat output for the space heating loop. For the domestic hot water loop, we used the output of the tank itself. Also, at times when the heat provided by the solar collectors is not enough, a heat resistance provides the auxiliary heating requirements to satisfy the energy needs.

The tank volume changes following a relation of 82.5 m^3 per m^2 of collector [23]. The tank height is a fixed value of 1.25 meters for the two cases of different solar collector area. Water is the fluid used for the tank and heat exchanger (HE) 2. For the HE 2, it enters the Tank at a fixed temperature of 30ºC meaning that from the higher output temperature needed (>50ºC), for space heating, the water doesn't transfer all its heat to the environment and instead the water stays warm. For the heat exchanger 1, a water based solution of 75% ethylene-glycol is used. The tank loss coefficient is given by 3 kJ h^{-1} m^{-2} K^{-1} and a fraction timestep of 6 is used on the tank.

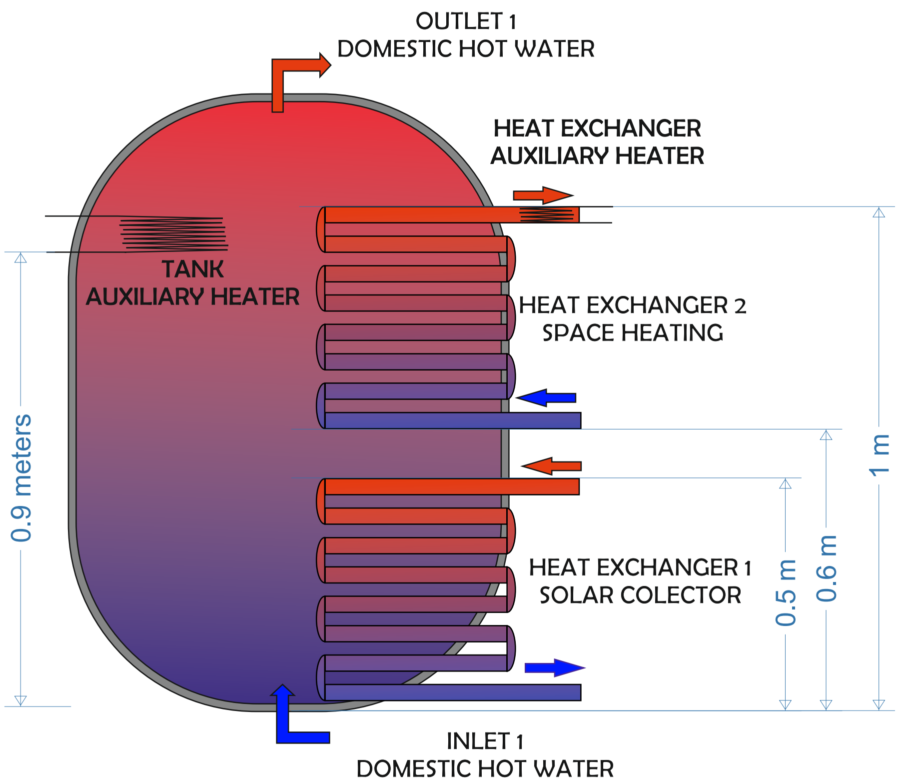

Figure 4.3: Scheme of the storage tank used and its inputs, outputs, heat exchangers and heights. Blue arrows represent cold fluid while red arrows represent hot fluid.

4.1.1.3 Solar Collector Loop

From fig. 4.1 in dark blue lines are represented the solar collector loop and its components: type109 (Weather), type3 (Pump), type2 (On-Off switch), solar collector type1 and Tank type60d. However, to test the different collector area, modifications have to be made the tank size, pump mass flow inlet, heat exchanger area and length, according to reference [23] and are presented in table 4.3.

The tank volume size must be 82.5 m^3 per m^2 of collector, the pump massflow is given by 0.02 kg s^{-1} per m^2 of STC [2], the heat exchanger surface area is give by 0.2 m^2 per m^2 of collector and the heat exchanger length is given by the area of a cylinder in equation 4.1.

$$A = \pi \cdot D \cdot L \tag{4.1}$$

- A, the total surface area of the heat exchanger in m^2
- D, the diameter = 0.012 m
- L, length of the heat exchanger in meters

[2]ISO 9806:2017 Solar energy – Solar thermal collectors – Test methods

Table 4.3: TRNSYS parameters modification when changing the collector area

Collector Area m^2	**Mass Flow Rate** kg hr^{-1}	**Tank Volume** m^3	**Heat Exchanger Length** m	**Total Surface Area of Heat Exchanger** m^2
4	288	330	21.20	0.8
6	432	495	31.85	1.2

The collector is a flat plate type with aperture area of 2.0 m^2 and displayed in table 4.4 are the values inserted in the component type.

The collector was positioned with a slope of 45º, 20% ground reflectance with the type using optical mode 2, meaning that the incidence angle modifier for adjustment is calculated following a second order quadratic function. The fluid used was a water based solution of 75% ethylene glycol with a specific heat of 2.93 kJ kg^{-1} m^{-2} K^{-1}. The solar fraction is given by eq. 4.2 and the solar collector thermal efficiency is given by equation 4.3. The intercept efficiency is corrected for non-nomal solar incidence by a modifying factor 4.4 with b_0 = 0.2 and b_1 = 0.

$$SolarFraction = \frac{Q_{STC} - Q_{TL}}{Q_{SH} + Q_{DHW}} \cdot 100 \tag{4.2}$$

$$\eta_{STC} = a_0 \cdot IAM - a_1 \frac{\Delta T}{I_T} - a_2 \frac{(\Delta T)^2}{I_T} \tag{4.3}$$

$$IAM = 1 - b_0 \cdot S - b_1 \cdot S^2 \quad with \quad S = \left(\frac{1}{cos(\theta)} - 1 \right) \tag{4.4}$$

For the control of the solar loop, the upper input temperature (T_{High}) is given by the

Table 4.4: Reference collector performance parameters from datasheet

$\mathbf{a_0}$	$\mathbf{a_1}$ kJ hr^{-1} m^{-2} K^{-1}	$\mathbf{a_2}$ kJ hr^{-1} m^{-2} K^{-2}
0.740	1.520	0.005

collector outlet temperature, the lower input temperature (T_{Low}) is given by the tank temperature at outlet of heat exchanger 1 and the monitoring temperature for high limit cut out checking is given by the temperature of outlet flow 1, as described in the storage tank figure 4.3. The lower dead band dT is given by 2K and the upper dead band dT by 10K. If the controller was previously ON and the lower dead band is smaller than the different of T_{High}-T_{Low}, then the controller remains ON. Otherwise it turns OFF. If the controller was previously OFF and the upper dead band value was smaller than T_{High}-T_{Low}, then the controller turns ON. Otherwise it remains OFF. Consult Appendix A figure A.2 for a scheme [22].

The monitoring temperature makes sure that no matter the result of the controller switch, the temperature never exceeds 100ºC for safety issues. Probable causes are collector stagnation and storage tank protection where the pump is not allowed to run if the tank temperature is above some prescribed limit. More details can be found in the reference [22] page 15.

4.1.1.4 Space Heating Loop

The space heating loop is represented with purple lines in fig. 4.1. We use 65ºC as the setpoint temperature from the outgoing HE2 of the tank and a return temperature of 30ºC. Knowing the heating rate required in the building to maintain 20ºC, we calculate what is the flow rate necessary with equation 4.5.

$$\dot{Q} = \dot{m} \cdot C_p \cdot (T_{setpoint} - T_{return}) \tag{4.5}$$

- $\dot{Q}$, heating rate in kJ hr^{-1}
- $\dot{m}$, mass flow rate in kg hr^{-1}
- C_p, specific heat for water in J kg^{-1} K^{-1}
- $T_{setpoint}$, exiting temperature in HE2 set point in ºC
- T_{return}, return temperature from the building central heating

Because there are situations when the tank can't give enough heat to maintain outgoing temperature of HE2 as 65ºC, a electric resistance will be simulated exclusively for the HE2. Using the same eq. 4.5, we can simulate the extra heating rate we must deliver to maintain the 65ºC set point but now the return temperature is given by the actual temperature exiting the heat exchanger 2 instead of the fixed 30ºC.

4.1.1.5 Water Draw Profile

Based on EU directive Number 814/2013 [1] and to simulate the usage of water in a single house family which uses in average 300 liters per day with different water draw-offs (tapping), the load profile M[3] was used. This was achieved in the TRNSYS environment using the 2 sets of four type14 components. One set simulates the profile mass flow and the other simulates the desired temperature for 0h-9h, 9h-15h, 15h-20h, 20h-24h timeframes of the day. The output connections "instantaneous water draw" from all 8 types are connected to the Diverter inputs "inlet mass flow rate" and "Set Point Temperature", respectively. If the "average water draw" output was used instead of the instantaneous water draw, the water used daily would be 213 liters instead of 315 liters. This is because the small timestep used during the simulation (90s) and the intervals of time in the load profile do not coincide, making TRNSYS average the value in the end of the simulation timestep instead of the actual time in the load profile.

The tapping cycle is defined as a set of the following parameters: heat demand per tapping (Q_{tap} [kWh]), minimum volume flow rate (f [l/min]), minimum temperature

[3] Found in annex III and table 1 of the directive [1]

(T_m [ºC]) and peak temperature (T_p [ºC]). Since the implementation in TRNSYS of this load profile requires different input values such as inlet and outlet temperatures and the mass flow rate, the profiles are recalculated based on the *Energy Labelling of Custom Built Systems*, *Deliverable D3.2* by Sebastian Bonk in QAiST[4] in Table 4.5 and presented in Appendix A Table A.2.

Table 4.5: Recalculations used to implement load profile on TRNSYS

Value	Calculation
Inlet Temperature (T_{CW})	10 ºC
Outlet Temperature (T_L)	During the tapping: max(T_m,T_p)
Mass Flow Rate (m_{dot})	$m_{dot} = \dfrac{Q_{tap}}{N \cdot dt \cdot cp \cdot (T_L - T_{CW})}$

With:

- N = discrete number of time steps
- dt = 90 seconds
- cp = 4.187 kJ kg^{-1} K^{-1}

Because the tank setpoint temperature is at 55ºC, a mixing valve is required to mix cold and hot water for domestic use at 30-45ºC (according to the load profile temperature requirements). This valve is simulated using two types 11 components: one as a tempering valve and another as a tee piece. The inlet temperature to mix the hot water is 10ºC. The types 14, simulating the load profile, connect to the diverter giving ON/OFF status and temperatures setpoints for the DHW. The temperature from storage tank outlet 1 connects to the heat source temperature of the diverter which then feeds back to the tank providing a flow rate and temperature for the tank inlet 1. Also, the diverter and the storage tank outlet 1 feeds the tee piece the flow and temperature of the water appropriated now for domestic use.

4.1.2 Photovoltaic project

In another TRNSYS project, a simple PV simulation system was used with photovoltaic panels (type94a) and the Data Reader and Radiation Processor component to read the weather data. Because of the architecture of the system used, the type94a didn't give all the outputs we required to make our Current-Voltage (IV) calculations curves. Using Compaq Visual Fortran Edition 6.6.B, license made available from LNEG, we altered the Proforma file so that we could get more outputs from our photovoltaic panel component, such as reverse saturation current dependent on temperature (I_{SAT}), photocurrent dependent on insolation (I_{PH}), cell temperature (TC), open circuit voltage (V_{OC}), short circuit

[4] http://www.qaist.org/

current (I_{SC}), fill factor (FF), series resistance (R_S), array voltage, array current, array power, power at maximum point (P_{MPP}), voltage at maximum point (V_{MPP}), current at maximum point (I_{MPP}), number of cells (N_S), number of modules in series (N_{MS}), number of modules in parallels (N_{MP}). This new type was called type161.

Each TRNSYS simulation ran for 8766 hours, simulating 1 year, with a time step of 1 hour and successive substitution as the solution method. The new component, type161, cell parameters were based on SUNPOWER[5] B50 Solar Cell G in mono crystalline silicon and the full data sheet can be found in appendix A fig. A.3. The cell parameters are in table 4.6.

Table 4.6: Electrical characteristics parameters of solar cell used from SUNPOWER, B50 Solar Cell G in mono crystalline silicon at standard test conditions: 1000W/m^2, AM 1.5 and cell temp 25ºC

V_{OC} V	I_{SC} A	V_{MPP} V	I_{MPP} A	P_{MPP} W	Efficiency %
0.664	5.72	0.557	5.33	2.97	20

4.2 Matlab System

4.2.1 PV-IV script

For each timestep of 1 hour in the TRNSYS simulation PV project, the function I.2 in annex I was created in MATLAB to calculate the PV-IV curve given the parameters: V_{OC}, I_{PH}, I_{SAT}, T_{AMB}, N_S, N_{MS}, N_{MP}, R_S, R_{SH}, A. The function can be summarized in:

- Start by creating a array sized 150 from 0 to V_{OC} and the start current i=0.
- A loop is created for each array element V(i).
- For each loop (idx), a current value I(idx) is calculated with equation 4.6 using the current from previous iteration (i).

$$I(idx) = I_{PH} - I_{SAT} \cdot \exp\left(\frac{V + (i \cdot R_S) \cdot q}{A \cdot k \cdot Tamb \cdot N_S}\right) - \frac{V + (i \cdot R_S)}{R_{SH}} \tag{4.6}$$

- In the end, the Tension array is multiplied by the number of cells and modules in series used in the simulation. The Current vector is multiplied by the number of modules in parallels.

[5] http://www.sunpowercorp.com

4.2.2 Methane production script

TRNSYS outputs from the photovoltaic project were saved in a .txt file and imported to MATLAB. These outputs are the characteristics parameters from a photovoltaic crystalline cell, that allow the construction of IV graph. The core script of this work is described in the scheme in the figure 4.4.

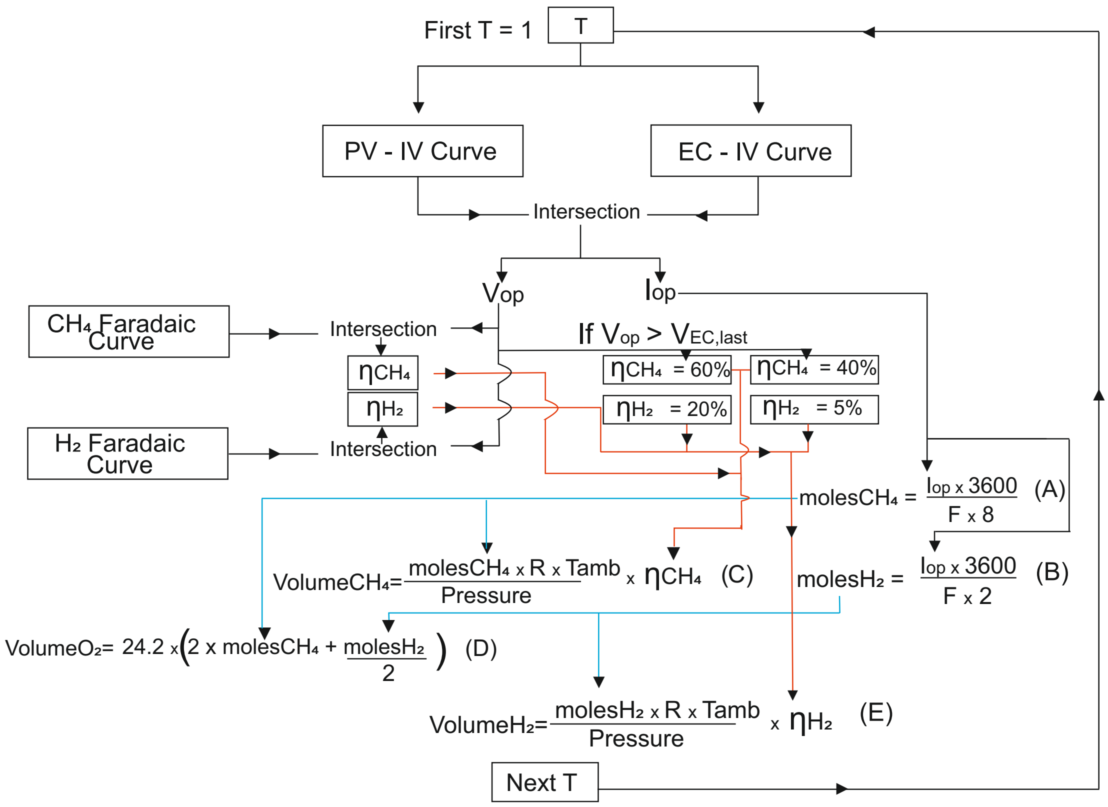

Figure 4.4: Scheme for the main MATLAB script. This is a loop for every hour of the yearly simulation, starting at iteration T=1. Vop in Volts, Iop in Amperes, F = 96485 Coulomb, R=0.082 atm/mole K, Tamb=298 K, Pressure = 1 atm.

The script calculates the methane produced hourly from the intersection of the photovoltaic panel's IV curve with the IV curve of a dispersible nanoscale copper catalyst[7] from Manthiram *et al* work. His group characterized this EC and the following curves from his article were used: Density of current vs Potential ([7] figure 2.A), CH_4 Faradaic Efficiency vs Potential ([7] figure 2.B) and H_2 Faradaic Efficiency vs Potential ([7] figure 2.D). Another assumption that was made for this simulation was that the performance of the electrodes was constant. To take deactivation into account a lower Faraday efficiency of 40% was considered. This deactivation is due, for example, to degradation of the n-Cu/C catalysts during the year. The size of the electrodes used in this thesis is given by 50cm x 50cm, which means a area equal to 0.25 m^2.

As shown in appendix B fig. B.17, *Manthiram et al.* experimental results Current Density vs Potential only reached -1.45 V vs RHE. As this data represents the potential of the cathode, we have estimated the whole cell potential adding 1.5 V for the anode reaction (oxygen evolution) considering an overpotential of ca. 0.3V. However, in some cases studied in the simulations, the voltage from PV-IV panel would be higher than 2.9 V as shown in 4.5. Assuming a constant selectivity of the reaction in this potential range, a fitting of the EC-IV and extrapolation until 4 V following equation $y = a \cdot e^{b+x}$ was created to take into account situations where the PV-IV wouldn't intersect with the EC-IV data. The code can be found in annex II.3. Also, in our calculations, CO_2 and water will never be the limiting factor in the reactions and only the power produced in the PV panels will limit our solar methane generation.

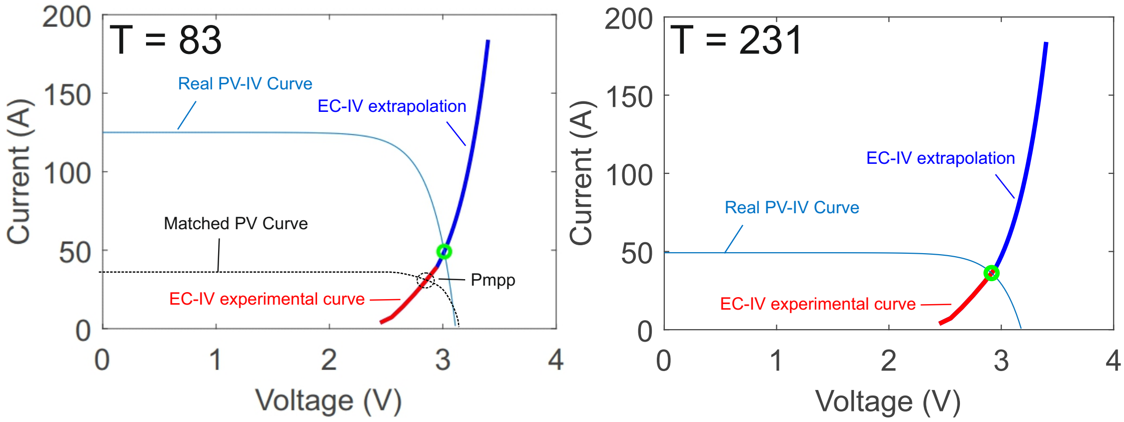

Figure 4.5: PV-IV intersecting with EC-IV for iteration T = 83 and T = 231 for the example case PV in Lisbon with 5 cells in series and 4 modules in parallel.

Ideally, the optimal point for intersection would be at P_{mpp} of the PV-IV curve. However, due to actual irradiance and temperature being the main parameters affecting the current variation, it is not easy and straightforward to find the optimal combination of cells and modules. A battery of tests with different configurations ranging from 1x1 (1 cell in series and 1 module in parallel) up to 12x12 (12 cells in series and 12 modules in parallel) was produced for the three different locations and then ran in the MATLAB script to oversee which configuration would produce more methane. The results are presented in appendix B. To have an idea on how the results deviate from the EC- IV experimental data, we calculated the percentage of incidence of those intersections on the extrapolated curve and found it satisfying considering results with less than 20% of intersections.

In the following code, the operational Current (I_{OP}), that resulted from the intersection of PV-IV with EC-IV, is multiplied by dt which represents 3600 seconds because each PV-IV curve is from 1 hour data. Because there are 8 electrons involved in CO_2RR cathodic reaction, eq. 4.8, each mole of CH_4 is given by dividing the product of Operational Current with dt per the product of Faraday constant with 8 (fig. 4.4 equation A).

```
        Farad = Iop(a) * dt * 1/F; % dt= 3600s , F = 96485 C/mol
        moleCH4 = Farad * 1/8;  % 8 electrons in the reaction
```

```
        VolumeCH4(a) = (moleCH4 * R * Tamb)/Pressao * etaCH4(a); % PV=nRT
        Metano = Metano + VolumeCH4(a);
```

By using the Ideal Gas Law $PV = nRT$ (fig. 4.4 eq. C), we can calculate the methane volume in liters produced for each hour. The value is then added to a summation variable to be printed at the end of the loop. The same principle is applied for the hydrogen production with the respective faradaic efficiency (fig. 4.4 equation B and E). The volume of oxygen produced at the anode (eq.4.7) can be calculated in the same way considering the total number of moles, formed in the reaction producing methane, and in the water electrolysis reaction (fig. 4.4 equation D).

$$Anodic : 2H_2O \rightarrow 4H^+ + 4e^- + O_2 \uparrow \tag{4.7}$$

$$\begin{aligned} Cathodic : &CO_2 + 8H^+ + 8e^- \rightarrow CH_4 + 2H_2O \\ &2H^+ + 2e^- \rightarrow H_2 \uparrow \end{aligned} \tag{4.8}$$

$$GlobalReaction : CO_2 + 2H_2O \rightarrow CH_4 + 2O_2 \tag{4.9}$$

4.3 Results

The results from the battery of tests for different PV panels configurations are presented in appendix B and the configuration chosen for each location took into consideration two parameters: maximum CH_4 production and less than 20% of results from the extrapolation curve. The latter percentage was arbitrarily chosen to minimize the number of intercepts with the extrapolation curve to lead to a conservative assumption of methane production.

In table 4.7 is summarized the production of Methane, Hydrogen and Oxygen for different locations taking into consideration that no electrode deactivation occurred. The columns of production are based on products produced per square meter of PV area per year. One module is a number of cells connected in series (N_S) and 1 PV unit is a number of modules connected in parallel (N_{MP}) as represented in the fig 4.6. We have also designated 1 EC unit as one electrode with geometrical area of 0.25 m^2.

Table 4.7: Methane, Hydrogen and Oxygen productions in Lisbon, Grenoble and Stockholm with electrocatalyst of 0.25 m^2 no deactivation considered. NTP conditions.

Location	**Ns**	**Nmp**	**PV Area m^2**	**CH_4 prod. kg/m$^2_{PV}$.y**	**H_2 prod. kg/m$^2_{PV}$.y**	**O_2 prod. kg/m$^2_{PV}$.y**	**Extrapolation Incidence Curve %**
Lisbon	12.0	12.0	2.250	16.8	2.8	223.1	17.9
Grenoble	10.0	12.0	1.875	14.7	2.4	195.4	14.9
Stockholm	10.0	12.0	1.875	12.5	2.1	166.2	12.0

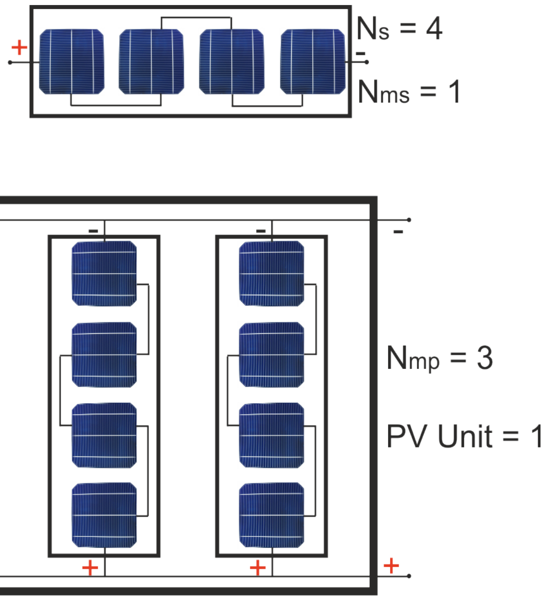

Figure 4.6: Scheme for the designated "PV Unit". In this example, 1 PV Unit consists of 4 cells connected in series are called 1 module. 3 Modules connected in parallel are called 1 PV Unit.

Appendix A and fig. A.1 show the radiation hitting the three different locations in study and Lisbon has the highest incidence with a mean radiation of 722 kJ/hr.m^2 followed by Grenoble with 545 kJ/hr.m^2 and finally Stockholm with 400 kJ/hr.m^2. As expected from this results, Lisbon would give a greater yield followed by Grenoble and Stockholm. Also, because of the higher irradiance in Lisbon and the temperature and irradiance being the actual parameters affecting methane production, we have more PV-IV EC-IV intersections in the extrapolation curve in relation to the other locations.

4.3.1 Influence of electrodes deactivation

To consider the effect of electrode deactivation, a faradaic efficiency of 40% was used when we get values on the extrapolation curve (>2.9V). As expected, a decrease in production of 33% is obtained, as presented in figure 4.7.

4.3.2 Influence of different space heating consumption

For the building in Grenoble and from fig. 4.8 we observe that heat demanded for domestic hot water are constant every month because this is not a random element embedded in the water profile and it repeats every 24 hours the same mass flow and temperature needed at the same time frames. We can also observe that in the summer months the heat supplied by the STC is doubled the one supplied in the winter and December is the month with a peak of energy demanded for SH by 800 kWh/month. From fig. 4.9 we can observe that in the same months that no space heating is required(May-August), there is also no need for auxiliary heating from the methane integrated system 4.9.

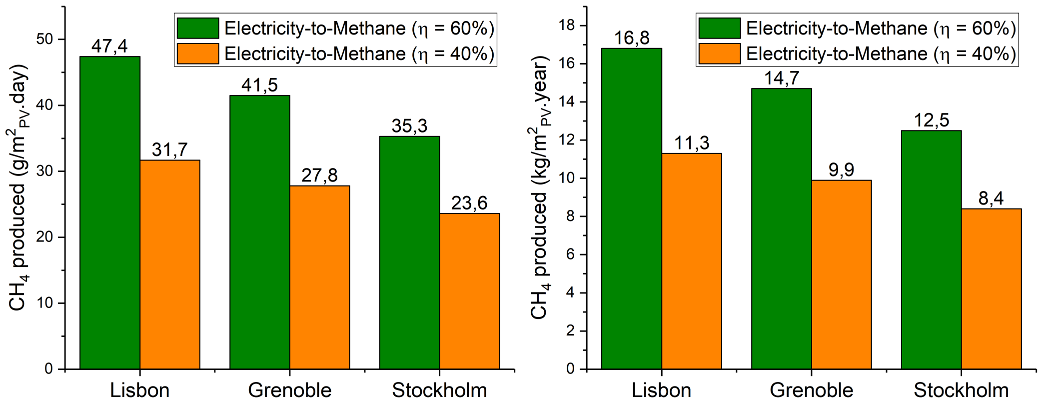

Figure 4.7: Left: Daily Methane Production Right: Yearly Methane Production

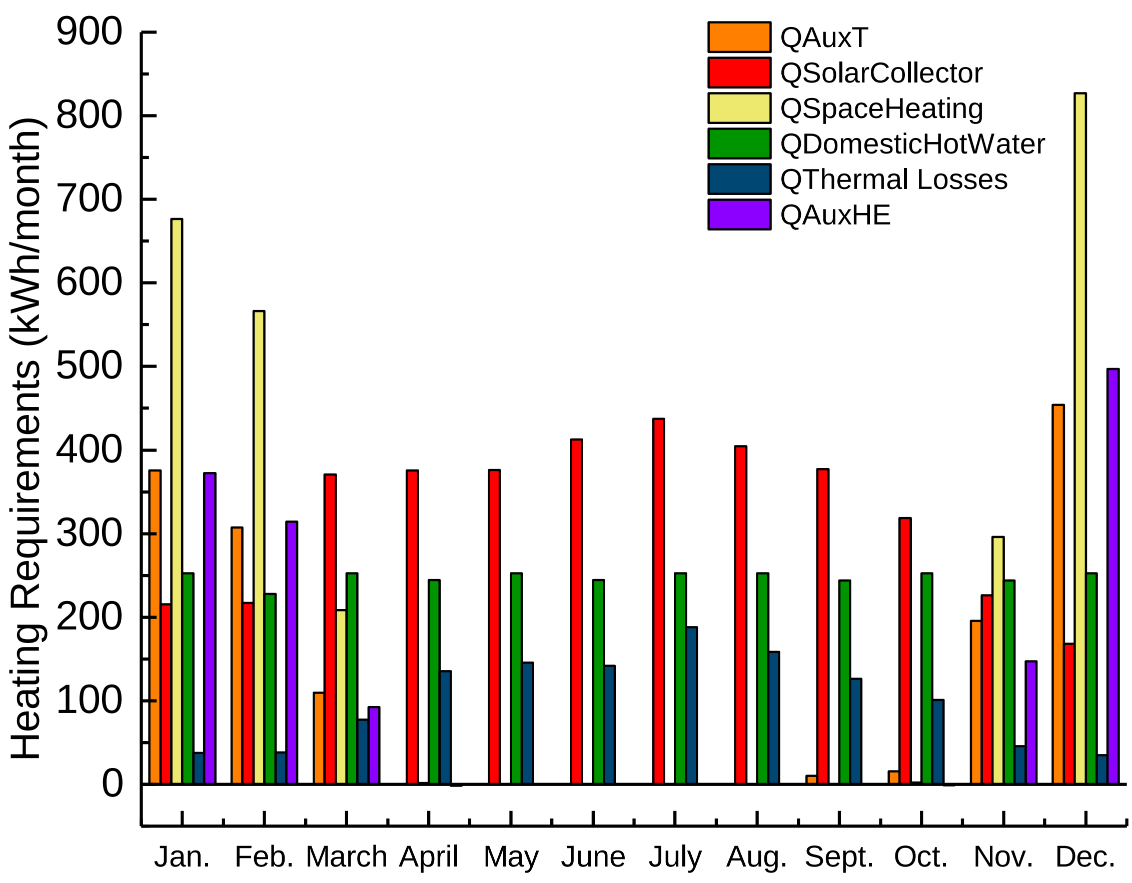

Figure 4.8: Monthly heating requirements for Grenoble building 15 kWh/m^2.year and STC 6 m^2

Increasing the space heating needs to 100 kWh/m^2 implies an increase in 20% of the fraction of QAux supplied. The heating load max is the maximum amount of energy supplied for space heating at a given moment. The buildings were designed to be as close as 15 and 100 kWh/m^2.year in space heating needs however it was not possible to reach exactly those requirements and so the effective space heating demand is presented in the table 4.8. Increasing in 460% the space heating demand provoked a demand for methane

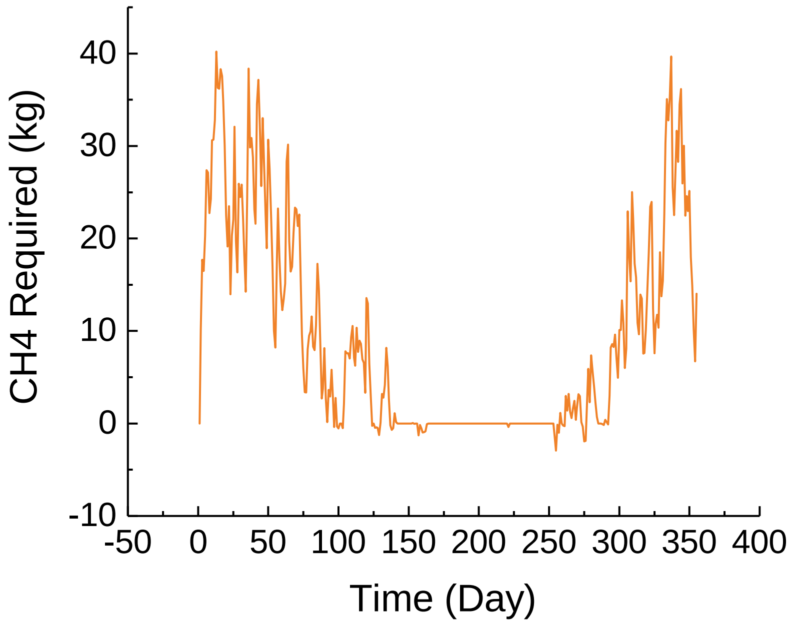

Figure 4.9: Daily methane requirements for Grenoble building 15 kWh/m^2.year and STC 6 m^2

increase in 360% for STC 4 m^2 and almost 400% for STC 6 m^2.

One PV unit is equal to 10 cells connected in series and 12 modules in parallel with a total area of 1.875 m^2 and one EC unit equals to a electrochemical reactor cell with an electrode geometrical area of 0.25 m^2. Using 1 Unit of PV and EC the system produces 27.7 and 18.5 kg of methane with η = 60 and 40% and taking into consideration a 90% methane combustion efficiency to heat. To fulfil the CH_4 requirements we would need several of those units, as represented in table 4.8. The auxiliary heating fraction is give by eq 4.10 and the methane needed for each situation takes into consideration a 90% combustion efficiency as it would burn in a conventional boiler.

Table 4.8: PV and EC area needed for Grenoble buildings. One PV Unit equals to 10 cells connected in series and 12 modules in parallel with a total area of 1.875 m^2. Solar Fraction + QAux Fraction = 100%

Building	STC m^2	η %	Area PV needed m^2	Area EC needed m^2	Number of EC & PV units	CH_4 needed kg/y	CH_4 generated per PV Unit kg/y	Solar Fraction %	Fraction QAux %	Heating Load Max kWh	Effective Space Heating demand kWh/m^2.y
bui15	4	60	17.8	2.4	9	262	27.7	41.0	59.0	50.0	18.5
		40	26.5	3.6	14		18.5				
	6	60	15.7	2.1	8	232	27.7	48.0	52.0		
		40	23.5	3.1	13		18.5				
bui100	4	60	81.7	10.9	44	1205	27.7	14.0	86.0	144.0	103.5
		40	122.1	16.3	65		18.5				
	6	60	77.6	10.4	41	1145	27.7	18.0	82.0		
		40	116.0	15.5	62		18.5				

$$FractionQAux = \frac{(Q_{AuxT} + Q_{AuxHE2})}{Q_{SH} + Q_{DHW}} \cdot 100 \tag{4.10}$$

4.3.3 Influence of different building location

Comparing Lisbon to Grenoble bui15, the number of Units needed decreased to feasible numbers with a best scenario requiring 7.5 m^2 of PV area and 8.4 m^2 of electrode geometrical area. However, when changing the location of the bui100 from Grenoble to Stockholm, the units needed increased from the minimum of 41 in Grenoble to a minimum of 53 in Stockholm, which represents a PV panel area of almost 100 m^2. In a situation with STC 6 m^2 and not considering electrodes deactivation on the EC, we can achieve the best result among te worst scenarios of about 95.3 m^2 PV area. The worst case scenario in Stockholm requires more PV panel area than the useful area of the building (140 m^2).

Table 4.9: PV and EC area needed for Lisbon building. One PV Unit equals to 12 cells connected in series and 12 modules in parallel with a total area of 2.25 m^2. Solar Fraction + QAux Fraction = 100%

Building	STC m^2	η %	Area PV needed m^2	Area EC needed m^2	Number of EC & PV units	CH_4 needed kg/y	CH_4 generated per PV Unit kg/y	Solar Fraction %	Fraction QAux %	Heating Load Max kWh	Effective Space Heating demand kWh/m^2.year
bui15	4	60.0	9.9	1.1	4	166.6	37.9	58.7	41.3	60.0	14.8
		40.0	14.8	1.6	7		25.3				
	6	60.0	7.5	0.8	3	127.0	37.9	68.5	31.5		
		40.0	11.3	1.3	5		25.3				

Table 4.10: PV and EC area needed for Stockholm building. One PV Unit equals to 10 cells connected in series and 12 modules in parallel with a total area of 1.875 m^2. Solar Fraction + QAux Fraction = 100%

Building	STC m^2	η %	Area PV needed m^2	Area EC needed m^2	Number of EC & PV units	CH_4 needed kg/y	CH_4 generated per PV Unit kg/y	Solar Fraction %	Fraction QAux %	Heating Load Max kWh	Effective Space Heating demand kWh/m^2.year
bui100	4	60	98.6	13.1	53	1236.7	23.5	10.4	89.6	157.0	101.7
		40	147.5	19.7	79		15.7				
	6	60	95.3	12.7	51	1195.1	23.5	13.4	86.6		
		40	142.5	18.9	76		15.7				

From fig. 4.11 we can observe that Stockholm lacks consistency, only producing in the summer months because that location has, in average, less than fifty hours of sunlight in january and in the peak of summer it has more than 300 hours (table 4.11). During those short sunlight in winter, the sun never reaches the altitude of the orientation of the PV panel (33º), because of that, no direct radiation is is focusing on the PV panel and consequently, no methane generation during the cold months. From table 4.11 and fig. 4.10 we can understand how the space heating demand increases in the winter but for those months, STCs and methane generation is limited by the number of sunshine hours provoking a increase by at least ten-fold compared to Lisbon in PV and EC units needed.

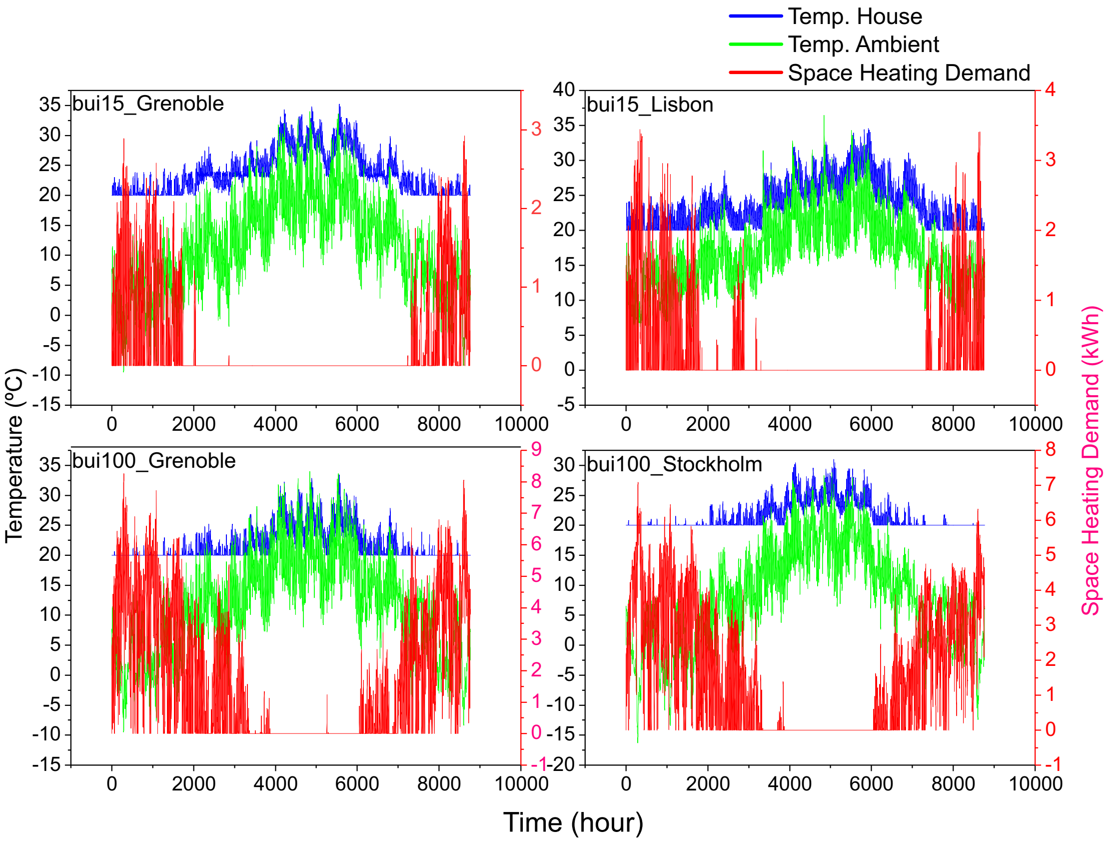

Figure 4.10: Building temperature, Ambient Temperature and Space Heating demand for 1 year in 3 locations

Table 4.11: Average Monthly sunlight hours in Lisbon, Grenoble and Stockholm in 2017, 2016 and 2016 [24–26]

Location	Sunlight hours per month											
	Jan.	Feb.	Mar.	April	May	June	July	August	Sept.	Oct.	Nov.	Dec.
Lisbon	150	180	200	250	390	325	395	350	285	200	180	160
Grenoble	75	120	175	175	200	230	275	225	190	160	100	70
Stockholm	50	75	150	200	300	315	300	250	180	100	50	40

4.3.4 Influence of different solar thermal collector area

Increasing the STC area from 4 m^2 to 6 m^2 has a greater impact in methane needs in Lisbon than in the other two locations with a decrease of 24% because of the increase in solar fraction from 58.8 to 68.5% for CS4 and CS6. It also shows a decrease of 25 and 22.6% in the energy supplied by the electric resistance in the tank and in the HE2. The CH_4 needed was calculated by summing the QAuxT and QAuxHE supplied energy, converting to kJ and knowing that methane has a energy density of 50 MJ/kg and a combustion efficiency of 90%.

The building in Grenoble is the one that has a increase more significant in the heat supplied by the solar collectors by 38.2%, however, this translates in a decrease of only

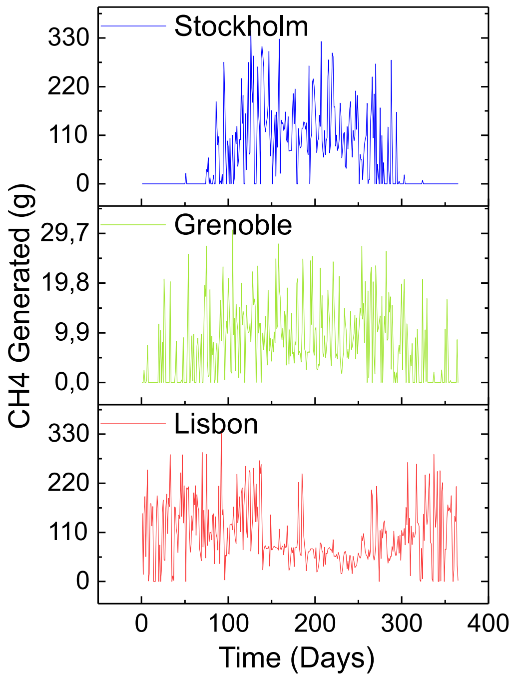

Figure 4.11: Methane daily production in Lisbon, Grenoble and Stockholm with 1 Unit of PV panel. No electrode deactivation.

Table 4.12: Percentual changes in energy demand and supplied with STC 6 m^2 in relation to STC 4 m^2

Building	Location	QAuxT %	QAuxHE %	QSTC %	QSH %	QDHW %	QTL %	CH4 Needed %
bui15	**Lisbon**	-25.0	-22.6	24.8	0.0	0.0	52.4	-24.0
	Grenoble	-15.6	-7.1	32.6	0.0	0.0	90.3	-11.9
bui100	**Grenoble**	-6.9	-4.1	38.2	0.0	0.0	76.5	-5.0
	Stockholm	-4.9	-2.6	37.0	0.0	0.0	74.5	-3.4

5% for methane demanded because at this stage the energy supplied by STCs is a order of magnitude lower than the energy demanded for space heating and the solar fraction is 14.1 and 18.3%, CS4 and CS6. For the building in Stockholm, quantity of methane needed was reduced by only 3.4%, which shows that increasing the STC in this location is not the best option to diminish the methane required because Stockholm the solar fraction increased by only 3%. In order to achieve better results for different locations we could change the slope of the STC depending on the location's latitude to increase direct sunlight energy.

From fig. 4.10 and appendix B tables for monthly results, we can conclude that the increase in thermal losses in every case, while increasing STCs area, is related to the extra energy supplied in the summer that is not needed for space heating or domestic hot water.

More detailed results can be found in appendix B.

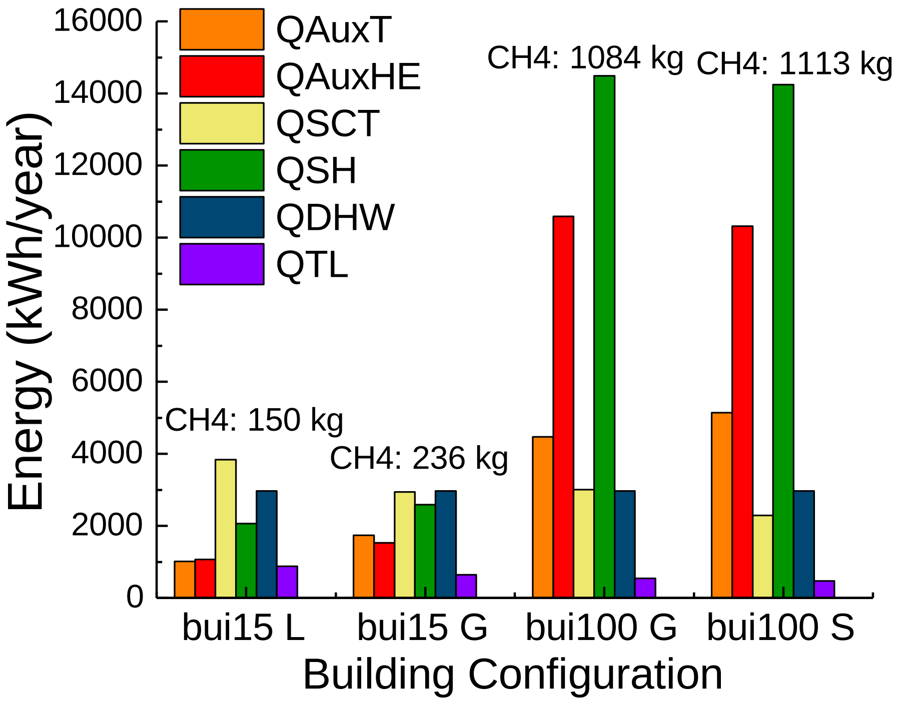

Figure 4.12: Energy supplied and demanded with STC 4 m^2. L stands for Lisbon location, G for Grenoble and S for Stockholm. QAuxT, QAuxHE and QSTC is supplied. QSH and SDHW is demanded. QTL are losses. Quantity of methane needed to satisfy heating requirements.

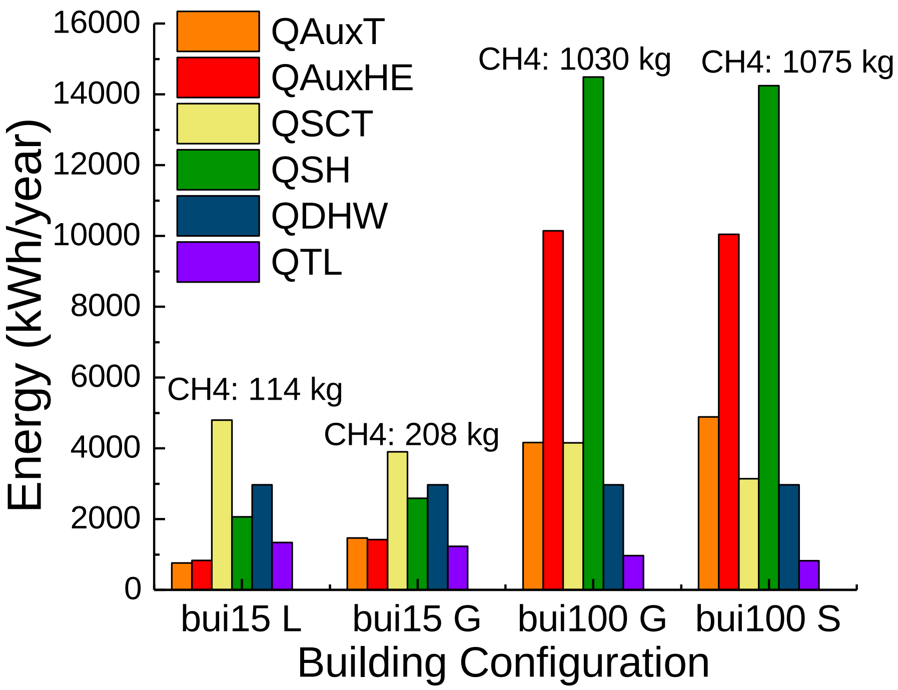

Figure 4.13: Energy supplied and demanded with STC 6 m^2. L stands for Lisbon location, G for Grenoble and S for Stockholm. QAuxT, QAuxHE and QSTC is supplied. QSH and SDHW is demanded. QTL are losses. Quantity of methane needed to satisfy heating requirements.

Chapter 5

Conclusion and future perspectives

In this work we approached a concept of a single house building with its heating requirements fulfilled by solar thermal collectors (STC) and solar methane produced by direct electrochemical reduction of carbon dioxide in an electrochemical cell (EC) powered by photovoltaic panels (PV). It must be beared in mind that this simulation work aims at integrating three technologies, PV, STC and EC. PV and STC are already commercial technologies but electrolytic methane production is still a low maturity, research technology. An intensive research effort is still necessary before this process can be deployed commercially.

The integrated technology was simulated in three different locations, Lisbon, Grenoble and Stockholm. The building in Lisbon presents clearly the highest methane production of 47.4 $g/{m_{PV}}^2$.day (0.658 kWh/day) and Stockholm the lowest 23.6 $g/{m_{PV}}^2$.day (0.328 kWh/day). The influence of the STC area was also studied. We can conclude that for Stockholm, the increase in STC area implies a decrease of 3% in methane needs, but in Lisbon this decrease was more significant (10%), because of the higher irradiance at lower latitudes. However, in real life situations we would get a decrease in production because of hydrogen competitive generation against methane and we would also get different byproducts because of inconsistent methane selectivity by today's state of the art technology.

Despite the fact that the buildings in Grenoble and Stockholm requires 100 kWh/m^2.y of space heating (bui100) need large PV areas to fulfil the energy requirements, the passive buildings seem more feasible in real life situations with PV areas around 10 m^2 in Lisbon and 20 m^2 in Grenoble. The simulation results also show that buildings in higher latitudes like in Stockholm cannot rely only on solar power, but they need to rely upon a mix of renewable energies, such as from wind and hydroelectric energies.

This simulation work could be extended in the future to take into account the method of CO_2 capture, the rate CO_2 recovery, type of equipments and their consumptions in order to make a economic viability study. In this work it was also not considered the amount of CH_4 produced in days with less space heating needs and excess methane generation. A full boiler connected to the tank instead of the electric resistance (QAuxT and QAuxHE) could be simulated coupled to a tank to store the excess of methane produced. With this approach, we could potentially see a decrease in PV and EC areas required, because we would have a buffer of methane for less sunny days and night periods. In order to maintain a smooth operation regardless of the inherent weather fluctuations, we could use a battery to store energy excess provided by the PV panels.

This simulation work relies on two main assumptions i) that a mature EC technology enables a stable electrode performance during the whole year (no significant electrode deactivation) and ii) high conversions of CO_2 into methane (>94%) so that a process for CH_4 purification requiring additional energy is not needed. Currently these assumptions are not met. Despite these limitations, this work shows the high potential of integration these technologies for a more sustainable way of living.

References

[1] European Comission. "COMMISION REGULATION (EU) No 814/2013." In: *Official Journal of the European Union* (2013).

[2] *What is a passive house*. Accessed on 10/9/2018. URL: https://passipedia.org/basics/what_is_a_passive_house.

[3] *Annual Global Carbon Emissions*. Accessed on 10/9/2018. URL: https://www.co2.earth/global-co2-emissions.

[4] M. R. Allen, D. J. Frame, C. Huntingford, C. D. Jones, J. A. Lowe, M. Meinshausen, and N. Meinshausen. "Warming caused by cumulative carbon emissions towards the trillionth tonne." In: *Nature* 458.7242 (2009), pp. 1163–1166. ISSN: 00280836. DOI: 10.1038/nature08019.

[5] L. Torrente-Murciano, D. Mattia, M. D. Jones, and P. K. Plucinski. "Formation of hydrocarbons via CO2hydrogenation - A thermodynamic study." In: *Journal of CO2 Utilization* 6 (2014), pp. 34–39. ISSN: 22129820. DOI: 10.1016/j.jcou.2014.03.002.

[6] J. Durst, A. Rudnev, A. Dutta, Y. Fu, J. Herranz, V. Kaliginedi, A. Kuzume, A. A. Permyakova, Y. Paratcha, P. Broekmann, and T. J. Schmidt. "Electrochemical CO2 Reduction – A Critical View on Fundamentals, Materials and Applications." In: *CHIMIA International Journal for Chemistry* 69.12 (2015), pp. 769–776. ISSN: 00094293. DOI: 10.2533/chimia.2015.769.

[7] K. Manthiram, B. J. Beberwyck, and A. P. Alivisatos. "Enhanced electrochemical methanation of carbon dioxide with a dispersible nanoscale copper catalyst." In: *Journal of the American Chemical Society* 136.38 (2014), pp. 13319–13325. ISSN: 15205126. DOI: 10.1021/ja5065284.

[8] I. Ganesh. "Electrochemical conversion of carbon dioxide into renewable fuel chemicals - The role of nanomaterials and the commercialization." In: *Renewable and Sustainable Energy Reviews* 59 (2016), pp. 1269–1297. ISSN: 18790690. DOI: 10.1016/j.rser.2016.01.026.

[9] Y. Hori, H. Konishi, T. Futamura, A. Murata, O. Koga, H. Sakurai, and K. Oguma. ""Deactivation of copper electrode"in electrochemical reduction of CO2." In: *Electrochimica Acta* 50.27 (2005), pp. 5354–5369. ISSN: 00134686. DOI: 10.1016/j.electacta.2005.03.015.

[10] H. Herzog. "Air Assessing the Feasibility of Capturing CO2 from the Air." In: *MIT Laboratory for Energy and the Environment* October (2003). ISSN: MIT LFEE 2003-002 WP.

[11] D. W. Keith, G. Holmes, D. St. Angelo, and K. Heidel. "A Process for Capturing CO2 from the Atmosphere." In: *Joule* 2.8 (2018), pp. 1573–1594. ISSN: 2542-4351. DOI: 10.1016/J.JOULE.2018.05.006.

[12] H. Tebibel, A. Khellaf, S. Menia, and I. Nouicer. "Design, modelling and optimal power and hydrogen management strategy of an off grid PV system for hydrogen production using methanol electrolysis." In: *International Journal of Hydrogen Energy* 42.22 (2017), pp. 14950–14967. ISSN: 03603199. DOI: 10.1016/j.ijhydene.2017.05.010.

[13] M. Schreier, L. Curvat, F. Giordano, L. Steier, A. Abate, S. M. Zakeeruddin, J. Luo, M. T. Mayer, and M. Grätzel. "Efficient photosynthesis of carbon monoxide from CO2 using perovskite photovoltaics." In: *Nature Communications* 6 (2015), p. 7326. ISSN: 2041-1723. DOI: 10.1038/ncomms8326.

[14] M. R. Singh, E. L. Clark, and A. T. Bell. "Thermodynamic and achievable efficiencies for solar-driven electrochemical reduction of carbon dioxide to transportation fuels." In: *Proceedings of the National Academy of Sciences of the United States of America* 112.45 (2015), E6111. ISSN: 00278424.

[15] F. Rossi, B. Castellani, E. Morini, L. D. Giovanna, N. Corsi, M. Giuliobello, and A. Nicolini. "Experimental apparatus for solar energy storage via methane production." In: *Third Southern African Solar Energy Conference* May (2014), pp. 341–346.

[16] A. L. Pisello, V. L. Castaldo, G. Pignatta, and F. Cotana. "14 th CIRIAF National Congress and cool pavement." In: September (2014).

[17] J. Guilera, J. Ramon Morante, and T. Andreu. "Economic viability of SNG production from power and CO2." In: *Energy Conversion and Management* 162.November 2017 (2018), pp. 218–224. ISSN: 01968904. DOI: 10.1016/j.enconman.2018.02.037.

[18] *Energy consumption in households.* Accessed on 10/9/2018. URL: https://ec.europa.eu/eurostat/statistics-explained/index.php/Energy_consumption_in_households.

[19] *Chemical Composition of Natural Gas.* Accessed on 10/9/2018. URL: https://www.uniongas.com/about-us/about-natural-gas/chemical-composition-of-natural-gas.

[20] *Heat Values of Various Fuels.* Accessed on 10/9/2018. URL: http://www.world-nuclear.org/information-library/facts-and-figures/heat-values-of-various-fuels.aspx.

[21] TRANSSOLAR, CSTB, TESS, SEL Univ. of Wisconsin-Madinson. *TRNSYS 16 - Volume 1 Getting Started.* 2005.

[22] TRANSSOLAR, CSTB, TESS, SEL Univ. of Wisconsin-Madinson. *TRNSYS 16 - Volume 5 Mathematical Reference*. 2005.

[23] F. A. Peuser. *Solar Thermal Systems: Successful Planning and Construction*. Routledge, 2011. ISBN: 9781849713313.

[24] *Monthly average sunlight hours in Lisbon for 2017*. Accessed on 2/10/2018. URL: https://weather-and-climate.com/average-monthly-Rainfall-Temperature-Sunshine,lisbon,Portugal.

[25] *Monthly average sunlight hours in Grenoble for 2016*. Accessed on 2/10/2018. URL: https://weather-and-climate.com/average-monthly-Rainfall-Temperature-Sunshine,grenoble,France.

[26] *Monthly average sunlight hours in Stockholm for 2016*. Accessed on 2/10/2018. URL: https://weather-and-climate.com/average-monthly-hours-Sunshine,Stockholm,Sweden.

[27] S. Bonk. "Energy Labelling of Custom Built Systems. Deliverable D3.5. Date: 26/05/2012. Final version. QAiST - Quality Assurance in Solar Heating and Cooling Technology." In: (2012), pp. 1–31.

[28] *Fast and Robust Curve Intersections*. Accessed on 4/4/2018. URL: https://www.mathworks.com/matlabcentral/fileexchange/11837-fast-and-robust-curve-intersections.

APPENDIX

A

Appendix: Supplementary data

Suplementary data that helps to understand this work.

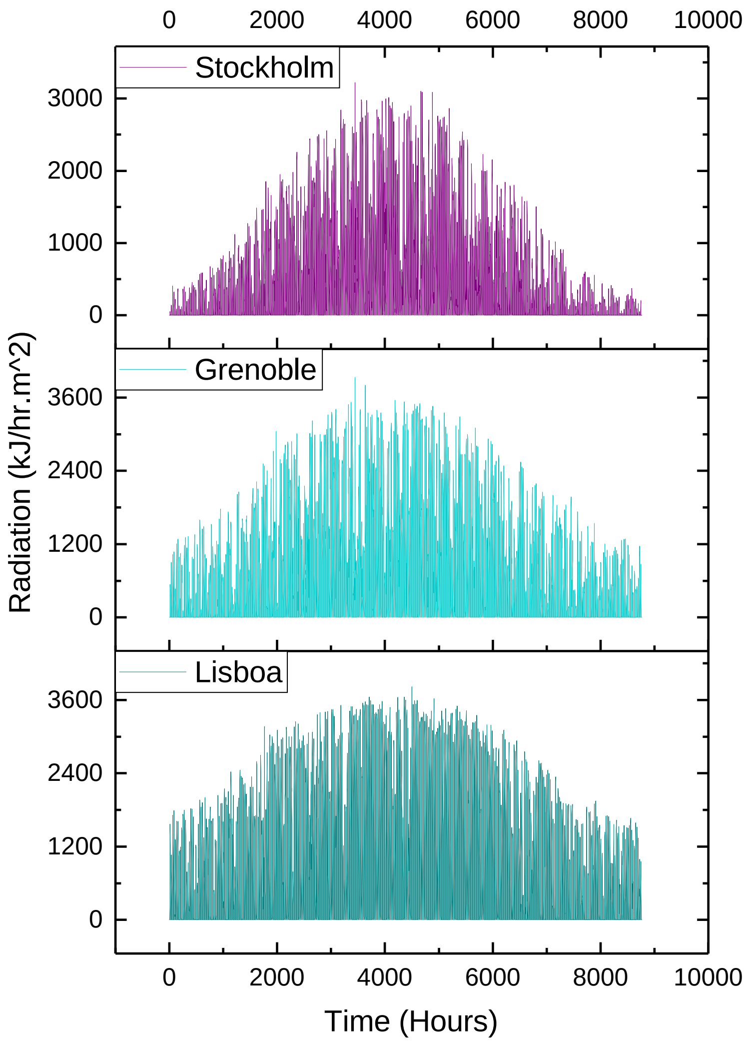

Figure A.1: Radiation values on a horizontal surface for Lisbon, Grenoble and Stockholm between 1991 and 2010 from Meteonorm.

Table A.1: MATLAB constants used in the functions and scripts developed

Name	Symbol	Value	Unit
Electron Charge	q	1.60E-19	C
Boltzman Constant	k	1.38E-23	$J\ K^{-1}$
Shunt Resistance	Rp	1.00E+06	Ohm
Faraday Constant	F	96485	$C\ mole^{-1}$
Gas constant	R	8.20E-02	$L\ atm\ mole^{-1}\ K^{-1}$
Pressure	p	1	atm
Ambient Temperature	Tamb	298	K
Methane Density (gas) NTP	ρ	0.668	$kg\ m^{-3}$
Oxygen Density (gas) NTP	ρ	1.331	$kg\ m^{-3}$
Hydrogen Density (gas) NTP	ρ	0.0827	$kg\ m^{-3}$
Oxygen Molar Mass	MO_2	1.60E+01	u

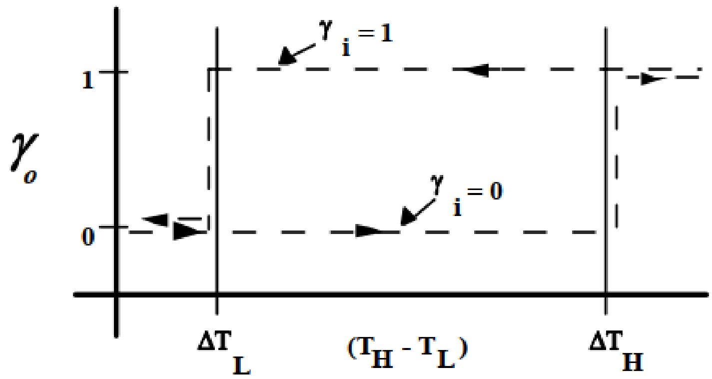

Figure A.2: Controller Function type2b. $\gamma 0$ is the output function value, 1 is ON, 0 is OFF. T_{Low} is lower input difference, T_{High} is upper input differente. $\Delta\ T_{Low}$ is lower dead band temperature difference and $\Delta\ T_{High}$ is upper dead band temperature difference. [22]

Table A.2: TRNSYS Load profile M [1] and implementation using Bonk [27] work.

Time	Extraction Duration s	N	Mass flow kg/hr	T_{CW} °C	T_L °C	m_{dot} kg/hr
07:00	120.372582	1	180	10	25	240.7452
07:05	401.241939	4	360	10	40	401.2419
07:15	0	0	0	10	0	0.0000
07:26	0	0	0	10	0	0.0000
07:30	120.372582	1	180	10	25	240.7452
07:45	0	0	0	10	0	0.0000
08:01	120.372582	1	180	10	25	240.7452
08:05	0	0	0	10	0	0.0000
08:15	120.372582	1	180	10	25	240.7452
08:25	0	0	0	10	0	0.0000
08:30	120.372582	1	180	10	25	240.7452
08:45	120.372582	1	180	10	25	240.7452
09:00	120.372582	1	180	10	25	240.7452
09:30	120.372582	1	180	10	25	240.7452
10:00	0	0	0	10	0	0.0000
10:30	60.1862909	1	180	10	40	120.3726
11:00	0	0	0	10	0	0.0000
11:30	120.372582	1	180	10	25	240.7452
11:45	120.372582	1	180	10	25	240.7452
12:00	0	0	0	10	0	0.0000
12:30	0	0	0	10	0	0.0000
12:45	90.2794364	1	240	10	55	240.7452
14:30	120.372582	1	180	10	25	240.7452
15:00	0	0	0	10	0	0.0000
15:30	120.372582	1	180	10	25	240.7452
16:00	0	0	0	10	0	0.0000
16:30	120.372582	1	180	10	25	240.7452
17:00	0	0	0	10	0	0.0000
18:00	120.372582	1	180	10	25	240.7452
18:15	60.1862909	1	180	10	40	120.3726
18:30	60.1862909	1	180	10	40	120.3726
19:00	120.372582	1	180	10	25	240.7452
19:30	0	0	0	10	0	0.0000
20:00	0	0	0	10	0	0.0000
20:30	210.652018	2	240	10	55	280.8694
20:45	0	0	0	10	0	0.0000
20:46	0	0	0	10	0	0.0000
21:00	0	0	0	10	0	0.0000
21:15	120.372582	1	180	10	25	240.7452
21:30	401.241939	4	360	10	40	401.2419
21:35	0	0	0	10	0	0.0000
21:45	0	0	0	10	0	0.0000

SUNPOWER

B50 SOLAR CELL

MONO CRYSTALLINE SILICON

Electrical Characteristics of Typical Cell at Standard Test Conditions (STC)

STC: 1000W/m², AM 1.5g and cell temp 25°C

Bin	Pmpp (Wp)	Eff. (%)	Vmpp (V)	Impp (A)	Voc (V)	Isc (A)
G	2.97	20.0	0.557	5.33	0.664	5.72
H	3.04	20.4	0.563	5.39	0.668	5.76
I	3.10	20.8	0.568	5.45	0.671	5.82
J	3.15	21.2	0.571	5.51	0.673	5.87

All Electrical Characteristics parameters are nominal
Unlaminated Cell Temperature Coefficients
Voltage: -1.8 mV / °C Power: -0.32% / °C

Positive Electrical Ground

Modules and systems produced using these cells must be configured as "positive ground systems".

TYPICAL I-V CURVE

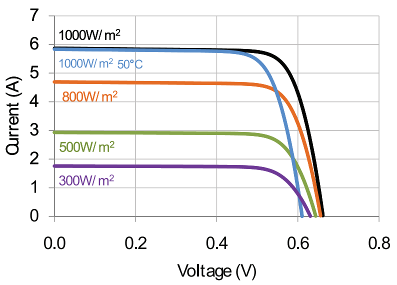

SPECTRAL RESPONSE

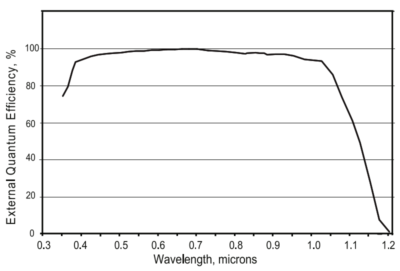

Physical Characteristics

Construction:	All back contact
Dimensions:	125mm x 125mm (nominal)
Thickness:	165μm ± 40μm
Diameter:	150mm (nominal)

Cell and Bond Pad Dimensions

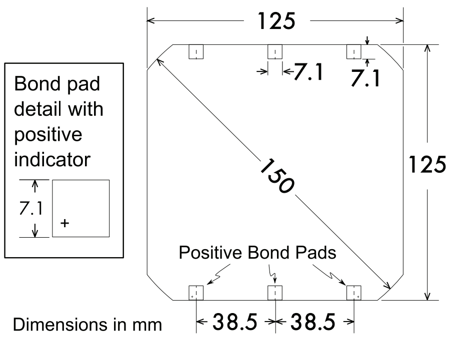

Bond pad area dimensions are 7.1mm x 7.1mm
Positive pole bond pad side has "+" indicator on leftmost and rightmost bond pads.

Interconnect Tab and Process Recommendations

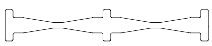

Tin plated copper interconnect. Compatible with lead free process.

Packaging

Cells are packed in boxes of 1,200 each; grouped in shrink-wrapped stacks of 150 with interleaving. Twelve boxes are packed in a water-resistant "Master Carton" containing 14,400 cells suitable for air transport.

Interconnect tabs are packaged in boxes of 1,200 each.

About SunPower

SunPower designs, manufactures, and delivers high-performance solar electric technology worldwide. Our high-efficiency solar cells generate up to 50 percent more power than conventional solar cells. Our high-performance solar panels, roof tiles, and trackers deliver significantly more energy than competing systems.

sunpowercorp.com

Document #001-66348 Rev*A A4_en

Figure A.3: Datasheet for B50 Solar Cell by SUNPOWER.

Appendix B

Appendix: Supplementary results

In this chapter we can find all the supplementary results that haven't been presented in the results chapter.

Table B.1: Influence on the energy supplied and demand with STC 4 m^2

Building	Location	QAuxT kWh/year	QAuxHE kWh/year	QSCT kWh/year	QSH kWh/year	QDHW kWh/year	QTL kWh/year	CH4 Needed kg/year
bui15	**Lisbon**	1011	1071	3841	2065	2970	881	150
	Grenoble	1741	1533	2940	2585	2970	646	236
bui100	**Grenoble**	4475	10585	3007	14487	2971	547	1084
	Stockholm	5142	10316	2289	14241	2971	470	1113

Table B.2: Influence on the energy supplied and demand with STC 6 m^2

Building	Location	QAuxT kWh/year	QAuxHE kWh/year	QSCT kWh/year	QSH kWh/year	QDHW kWh/year	QTL kWh/year	CH4 Needed kg/year
bui15	**Lisbon**	758	829	4793	2065	2970	1343	114
	Grenoble	1470	1424	3899	2585	2971	1231	208
bui100	**Grenoble**	4164	10146	4155	14487	2971	966	1030
	Stockholm	4890	10049	3137	14241	2972	819	1075

Table B.3: Methane production (kg) in Lisbon with η = 60% with different PV panels configurations

parallels \ series	1	2	3	4	5	6	7	8	9	10	11	12
1	0.0	0.0	0.0	0.0	0.3	0.5	0.6	0.6	0.5	0.5	0.4	0.4
2	0.0	0.0	0.0	0.0	1.1	2.1	2.4	2.5	2.4	2.3	2.1	2.0
3	0.0	0.0	0.0	0.0	1.8	3.3	4.2	4.5	4.5	4.4	4.2	3.9
4	0.0	0.0	0.0	0.1	2.2	4.5	6.2	7.0	7.2	7.1	6.8	6.4
5	0.0	0.0	0.0	0.1	2.5	5.6	8.3	9.8	10.4	10.4	10.0	9.6
6	0.0	0.0	0.0	0.1	2.7	6.7	10.6	12.9	13.9	14.1	13.8	13.2
7	0.0	0.0	0.0	0.1	2.8	7.7	12.9	16.2	17.8	18.2	17.9	17.3
8	0.0	0.0	0.0	0.1	2.9	8.6	15.2	19.7	22.0	22.7	22.6	21.9
9	0.0	0.0	0.0	0.0	3.0	9.5	17.5	23.3	26.4	27.6	27.6	26.9
10	0.0	0.0	0.0	0.0	3.0	10.2	19.8	27.1	31.2	32.9	33.1	32.4
11	0.0	0.0	0.0	0.0	3.0	10.9	22.1	31.0	36.2	38.4	38.7	37.8
12	0.0	0.0	0.0	0.0	3.0	11.5	24.4	35.0	41.0	42.6	42.3	40.6

Table B.4: Methane production (kg) in Lisbon with η = 40% with different PV panels configurations

parallels \ series	1	2	3	4	5	6	7	8	9	10	11	12
1	0.0	0.0	0.0	0.0	0.3	0.5	0.6	0.6	0.5	0.5	0.4	0.4
2	0.0	0.0	0.0	0.0	1.1	2.0	2.2	2.2	2.1	2.0	1.9	1.8
3	0.0	0.0	0.0	0.0	1.8	2.7	3.2	3.3	3.3	3.2	3.1	2.9
4	0.0	0.0	0.0	0.1	2.1	3.4	4.4	4.9	5.1	5.0	4.8	4.5
5	0.0	0.0	0.0	0.1	2.3	4.1	5.8	6.8	7.2	7.1	6.9	6.6
6	0.0	0.0	0.0	0.1	2.4	4.8	7.3	8.8	9.5	9.6	9.4	9.0
7	0.0	0.0	0.0	0.1	2.5	5.5	8.8	11.0	12.0	12.3	12.1	11.7
8	0.0	0.0	0.0	0.1	2.5	6.1	10.3	13.3	14.8	15.3	15.2	14.7
9	0.0	0.0	0.0	0.0	2.5	6.6	11.9	15.7	17.8	18.6	18.6	18.1
10	0.0	0.0	0.0	0.0	2.5	7.1	13.4	18.2	20.9	22.0	22.2	21.7
11	0.0	0.0	0.0	0.0	2.5	7.5	14.9	20.8	24.2	25.7	25.9	25.3
12	0.0	0.0	0.0	0.0	2.4	7.9	16.4	23.5	27.5	28.5	28.3	27.2

Table B.5: Incidence curves (%) for methane production in Lisbon with different PV panels configurations

parallels \ series	1	2	3	4	5	6	7	8	9	10	11	12
1	0.0	0.0	0.0	0.0	0.0	0.0	0.0	0.0	0.0	0.0	0.0	0.0
2	0.0	0.0	0.0	0.0	0.0	0.9	3.4	4.2	4.3	4.0	3.5	3.0
3	0.0	0.0	0.0	0.0	0.3	7.8	10.8	11.8	11.8	11.3	10.6	10.0
4	0.0	0.0	0.0	0.0	1.8	11.1	14.1	14.7	14.5	14.0	13.4	12.7
5	0.0	0.0	0.0	0.0	3.5	13.0	15.6	16.2	16.0	15.5	14.9	14.2
6	0.0	0.0	0.0	0.0	4.5	14.1	16.7	17.4	17.3	16.7	16.1	15.3
7	0.0	0.0	0.0	0.0	5.4	15.1	17.8	18.5	18.2	17.7	17.1	16.3
8	0.0	0.0	0.0	0.0	6.0	15.9	18.4	19.1	18.9	18.4	17.8	17.0
9	0.0	0.0	0.0	0.0	6.4	16.6	19.0	19.6	19.4	19.0	18.3	17.5
10	0.0	0.0	0.0	0.0	6.8	17.0	19.5	20.0	19.8	19.4	18.7	17.9
11	0.0	0.0	0.0	0.0	7.1	17.4	19.7	20.3	20.1	19.7	19.0	18.1
12	0.0	0.0	0.0	0.0	7.3	17.6	20.0	20.6	20.3	19.7	18.8	17.9

Table B.6: Methane production (kg) in Grenoble with η = 60% with different PV panels configurations

parallels \ series	1	2	3	4	5	6	7	8	9	10	11	12
1	0.0	0.0	0.0	0.0	0.2	0.3	0.4	0.4	0.3	0.3	0.3	0.2
2	0.0	0.0	0.0	0.0	0.8	1.4	1.6	1.7	1.6	1.5	1.5	1.4
3	0.0	0.0	0.0	0.1	1.4	2.3	2.9	3.1	3.1	3.1	2.9	2.8
4	0.0	0.0	0.0	0.1	1.7	3.3	4.4	4.9	5.1	5.0	4.9	4.6
5	0.0	0.0	0.0	0.1	2.0	4.2	6.0	7.0	7.3	7.4	7.2	6.9
6	0.0	0.0	0.0	0.1	2.2	5.1	7.7	9.2	9.9	10.1	9.9	9.5
7	0.0	0.0	0.0	0.1	2.3	6.0	9.5	11.7	12.8	13.1	12.9	12.6
8	0.0	0.0	0.0	0.1	2.4	6.8	11.3	14.3	15.9	16.4	16.4	15.9
9	0.0	0.0	0.0	0.1	2.5	7.6	13.2	17.1	19.2	20.0	20.1	19.7
10	0.0	0.0	0.0	0.1	2.6	8.4	15.1	20.0	22.8	23.9	24.1	23.7
11	0.0	0.0	0.0	0.0	2.6	9.1	17.1	23.0	26.4	27.3	27.1	26.6
12	0.0	0.0	0.0	0.0	2.6	9.7	19.0	26.1	29.0	29.6	29.4	28.6

Table B.7: Methane production (kg) in Grenoble with η = 40% with different PV panels configurations

parallels \ series	1	2	3	4	5	6	7	8	9	10	11	12
1	0.0	0.0	0.0	0.0	0.2	0.3	0.4	0.4	0.3	0.3	0.3	0.2
2	0.0	0.0	0.0	0.0	0.8	1.3	1.5	1.5	1.4	1.4	1.3	1.2
3	0.0	0.0	0.0	0.1	1.3	2.0	2.2	2.4	2.4	2.3	2.2	2.1
4	0.0	0.0	0.0	0.1	1.6	2.5	3.2	3.5	3.6	3.5	3.4	3.3
5	0.0	0.0	0.0	0.1	1.8	3.1	4.2	4.8	5.1	5.1	4.9	4.7
6	0.0	0.0	0.0	0.1	1.9	3.7	5.3	6.3	6.8	6.8	6.7	6.5
7	0.0	0.0	0.0	0.1	2.0	4.2	6.5	7.9	8.6	8.8	8.8	8.5
8	0.0	0.0	0.0	0.1	2.0	4.8	7.7	9.7	10.7	11.1	11.0	10.7
9	0.0	0.0	0.0	0.1	2.1	5.3	9.0	11.5	12.9	13.5	13.5	13.2
10	0.0	0.0	0.0	0.1	2.1	5.7	10.2	13.4	15.3	16.1	16.2	15.9
11	0.0	0.0	0.0	0.0	2.1	6.2	11.5	15.5	17.7	18.3	18.1	17.8
12	0.0	0.0	0.0	0.0	2.1	6.6	12.8	17.5	19.4	19.8	19.7	19.1

Table B.8: Incidence curves (%) for methane production in Grenoble with different PV panels configurations

parallels \ series	1	2	3	4	5	6	7	8	9	10	11	12
1	0.0	0.0	0.0	0.0	0.0	0.0	0.0	0.0	0.0	0.0	0.0	0.0
2	0.0	0.0	0.0	0.0	0.0	0.8	1.9	2.5	2.6	2.4	2.1	1.9
3	0.0	0.0	0.0	0.0	0.5	5.0	7.2	7.7	7.7	7.3	7.1	6.7
4	0.0	0.0	0.0	0.0	1.8	8.1	10.0	10.4	10.3	10.1	9.7	9.3
5	0.0	0.0	0.0	0.0	3.1	9.8	11.6	12.0	12.0	11.7	11.3	11.0
6	0.0	0.0	0.0	0.0	3.9	10.9	12.8	13.1	13.1	12.8	12.4	12.1
7	0.0	0.0	0.0	0.0	4.5	11.8	13.5	13.9	13.8	13.5	13.1	12.8
8	0.0	0.0	0.0	0.0	5.0	12.5	14.1	14.5	14.4	14.1	13.6	13.3
9	0.0	0.0	0.0	0.0	5.5	12.9	14.4	14.8	14.7	14.4	13.9	13.6
10	0.0	0.0	0.0	0.0	5.9	13.3	14.8	15.2	15.1	14.8	14.3	14.0
11	0.0	0.0	0.0	0.0	6.1	13.5	15.1	15.5	15.4	15.0	14.5	14.2
12	0.0	0.0	0.0	0.0	6.3	13.7	15.3	15.7	15.4	14.9	14.4	14.0

Table B.9: Methane production (kg) in Stockholm with η = 60% with different PV panels configurations

parallels \ series	1	2	3	4	5	6	7	8	9	10	11	12
1	0.0	0.0	0.0	0.0	0.1	0.3	0.3	0.3	0.3	0.2	0.2	0.2
2	0.0	0.0	0.0	0.0	0.7	1.1	1.3	1.3	1.3	1.2	1.2	1.1
3	0.0	0.0	0.0	0.0	1.1	1.9	2.4	2.6	2.6	2.5	2.4	2.3
4	0.0	0.0	0.0	0.0	1.5	2.7	3.6	4.1	4.2	4.2	4.1	3.9
5	0.0	0.0	0.0	0.1	1.7	3.5	5.0	5.8	6.1	6.2	6.1	5.9
6	0.0	0.0	0.0	0.1	1.8	4.2	6.4	7.7	8.3	8.5	8.4	8.1
7	0.0	0.0	0.0	0.1	2.0	5.0	7.9	9.8	10.8	11.1	11.0	10.8
8	0.0	0.0	0.0	0.1	2.1	5.7	9.5	12.1	13.4	14.0	14.0	13.7
9	0.0	0.0	0.0	0.0	2.1	6.3	11.1	14.5	16.3	17.1	17.2	16.9
10	0.0	0.0	0.0	0.0	2.2	6.9	12.7	16.9	19.3	20.4	20.6	20.3
11	0.0	0.0	0.0	0.0	2.2	7.5	14.3	19.5	22.5	23.4	23.3	23.0
12	0.0	0.0	0.0	0.0	2.2	8.1	15.9	22.0	24.9	25.2	25.0	24.4

Table B.10: Methane production (kg) in Stockholm with η = 40% with different PV panels configurations

parallels \ series	1	2	3	4	5	6	7	8	9	10	11	12
1	0.0	0.0	0.0	0.0	0.1	0.3	0.3	0.3	0.3	0.2	0.2	0.2
2	0.0	0.0	0.0	0.0	0.7	1.1	1.2	1.2	1.1	1.1	1.0	1.0
3	0.0	0.0	0.0	0.0	1.1	1.6	1.8	1.9	1.9	1.9	1.8	1.7
4	0.0	0.0	0.0	0.0	1.4	2.1	2.6	2.9	3.0	3.0	2.9	2.8
5	0.0	0.0	0.0	0.1	1.5	2.5	3.5	4.0	4.2	4.3	4.2	4.0
6	0.0	0.0	0.0	0.1	1.6	3.0	4.4	5.3	5.7	5.8	5.7	5.5
7	0.0	0.0	0.0	0.1	1.7	3.4	5.4	6.7	7.3	7.5	7.4	7.3
8	0.0	0.0	0.0	0.1	1.7	3.9	6.5	8.2	9.0	9.4	9.4	9.2
9	0.0	0.0	0.0	0.0	1.7	4.3	7.5	9.7	10.9	11.5	11.5	11.3
10	0.0	0.0	0.0	0.0	1.8	4.7	8.6	11.4	13.0	13.7	13.8	13.6
11	0.0	0.0	0.0	0.0	1.8	5.1	9.6	13.1	15.1	15.6	15.6	15.4
12	0.0	0.0	0.0	0.0	1.7	5.5	10.7	14.8	16.7	16.9	16.7	16.3

Table B.11: Incidence curves (%) for methane production in Stockholm with different PV panels configurations

parallels \ series	1	2	3	4	5	6	7	8	9	10	11	12
1	0.0	0.0	0.0	0.0	0.0	0.0	0.0	0.0	0.0	0.0	0.0	0.0
2	0.0	0.0	0.0	0.0	0.0	0.7	1.8	2.3	2.4	2.3	2.1	1.9
3	0.0	0.0	0.0	0.0	0.3	4.5	5.9	6.1	6.1	6.0	5.8	5.5
4	0.0	0.0	0.0	0.0	1.4	6.7	7.9	8.2	8.1	8.0	7.8	7.6
5	0.0	0.0	0.0	0.0	2.5	8.4	9.4	9.7	9.6	9.5	9.2	9.0
6	0.0	0.0	0.0	0.0	3.3	9.6	10.5	10.8	10.7	10.5	10.3	10.1
7	0.0	0.0	0.0	0.0	4.0	10.2	11.0	11.3	11.2	11.0	10.8	10.6
8	0.0	0.0	0.0	0.0	4.4	10.6	11.4	11.7	11.6	11.4	11.2	11.0
9	0.0	0.0	0.0	0.0	4.8	10.9	11.7	12.0	11.9	11.7	11.5	11.3
10	0.0	0.0	0.0	0.0	5.0	11.1	12.0	12.3	12.2	12.0	11.8	11.5
11	0.0	0.0	0.0	0.0	5.3	11.4	12.3	12.5	12.4	12.1	11.9	11.6
12	0.0	0.0	0.0	0.0	5.5	11.5	12.4	12.7	12.4	12.0	11.7	11.4

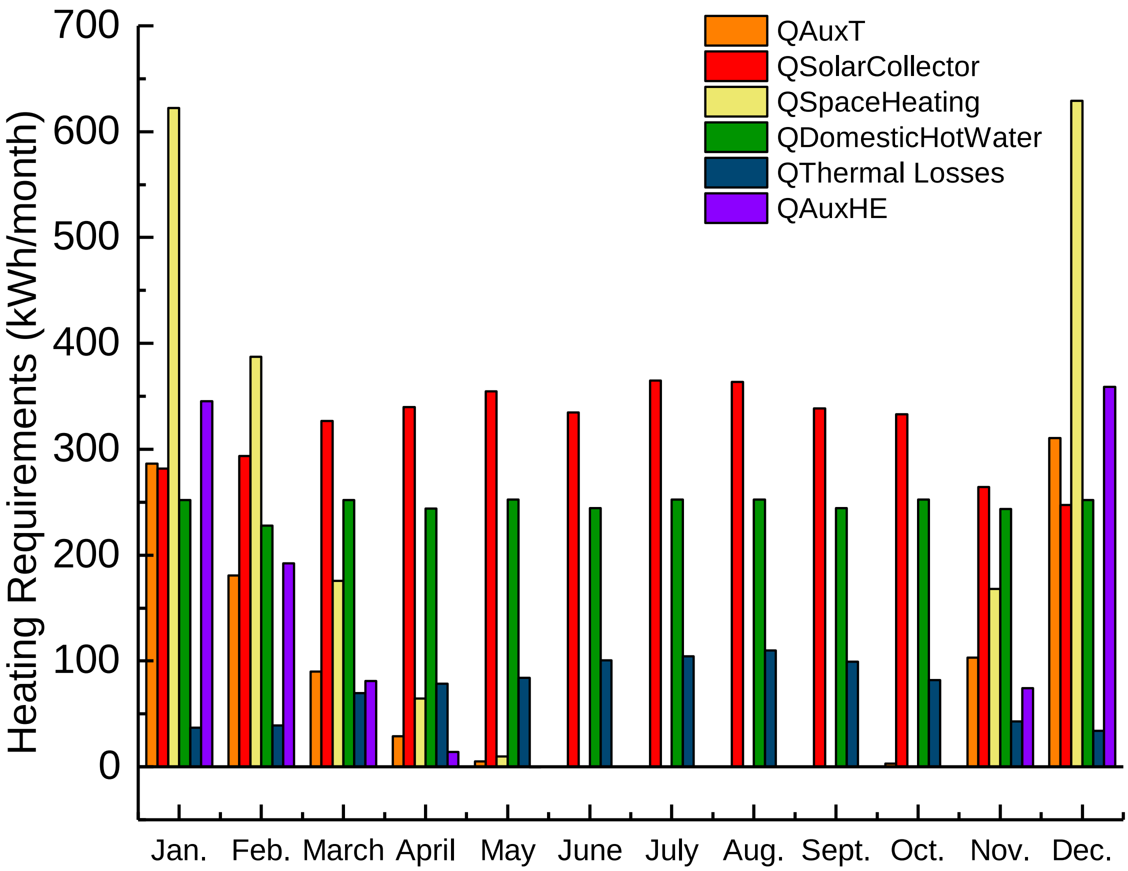

Figure B.1: Monthly heating requirements for Lisboa building 15 kWh/m^2.year and STC 4 m^2

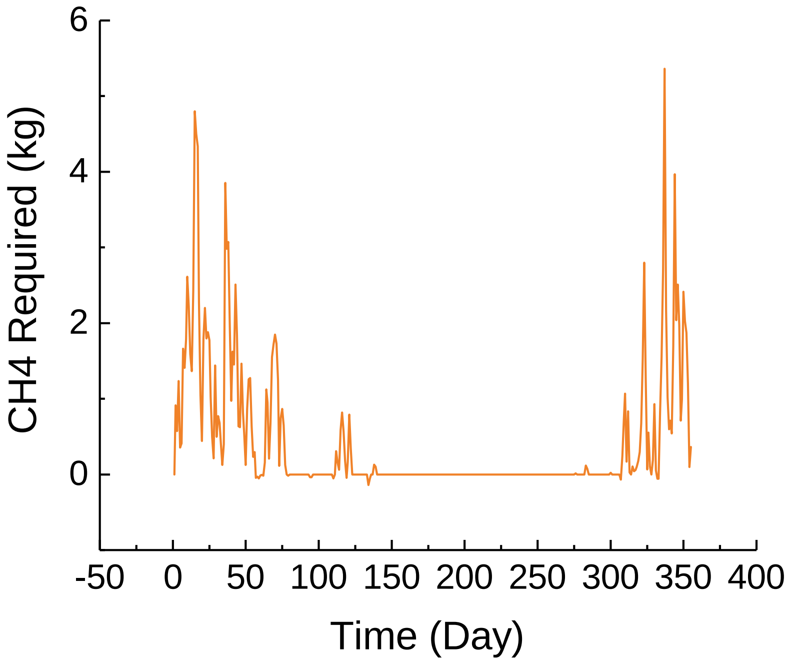

Figure B.2: Daily methane requirements for Lisboa building 15 kWh/m^2.year and STC 4 m^2

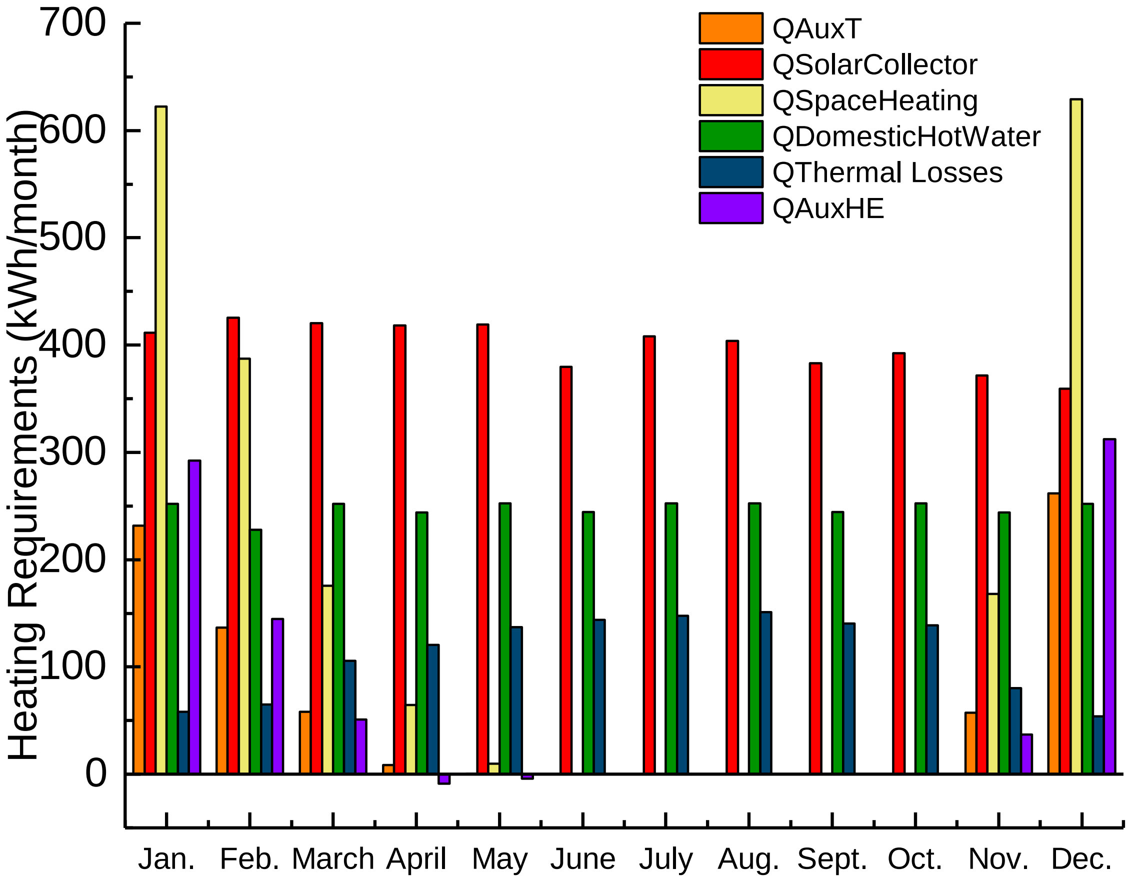

Figure B.3: Monthly heating requirements for Lisboa building 15 kWh/m^2.year and STC 6 m^2

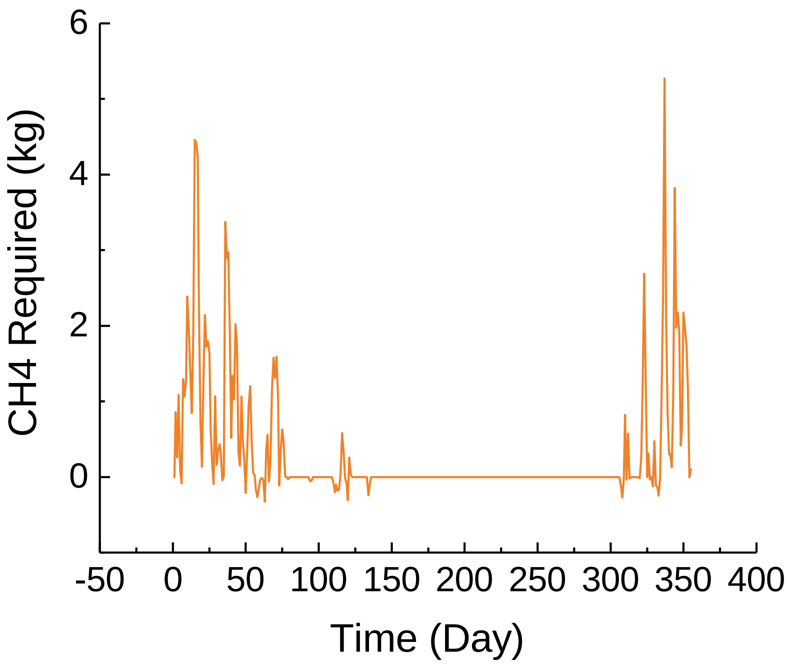

Figure B.4: Daily methane requirements for Lisboa building 15 kWh/m^2.year and STC 6 m^2

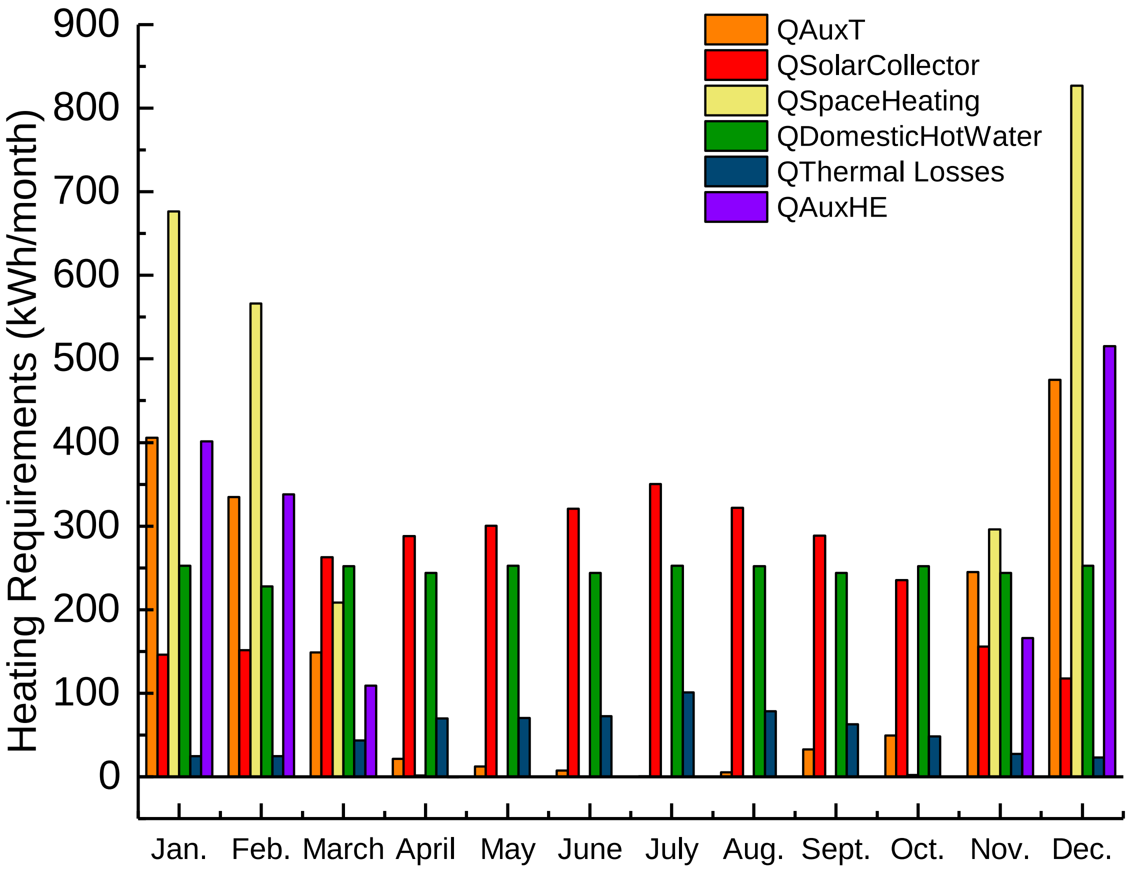

Figure B.5: Monthly heating requirements for Grenoble building 15 kWh/m^2.year and STC 4 m^2

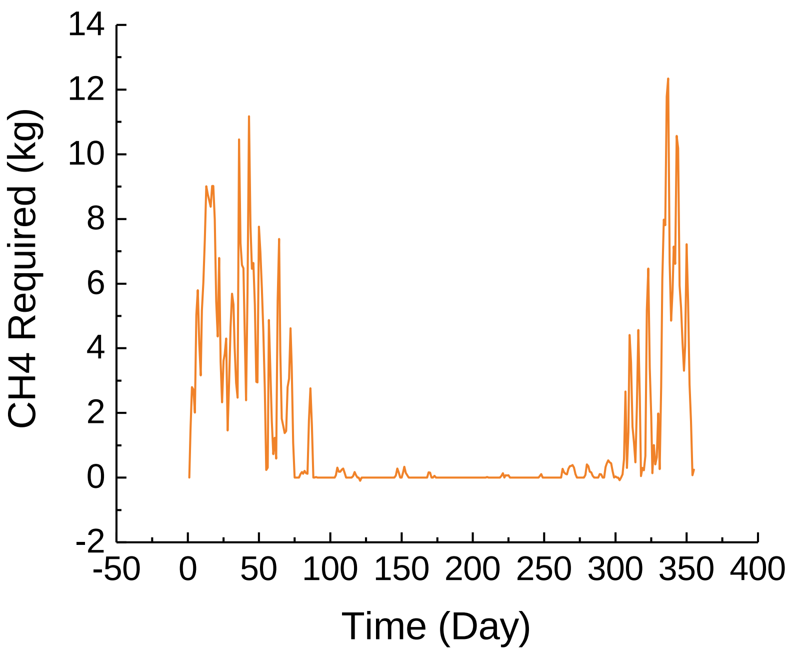

Figure B.6: Daily methane requirements for Grenoble building 15 kWh/m^2.year and STC 4 m^2

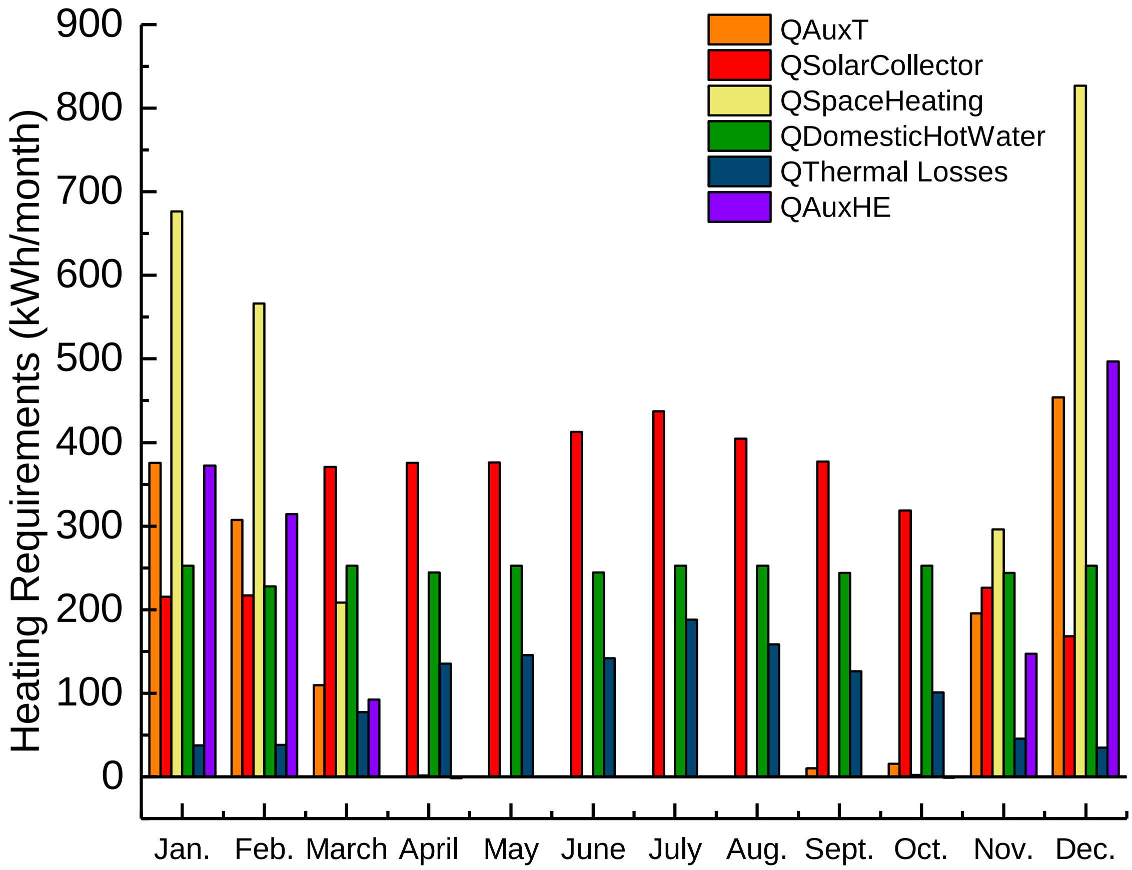

Figure B.7: Monthly heating requirements for Grenoble building 15 kWh/m^2.year and STC 6 m^2

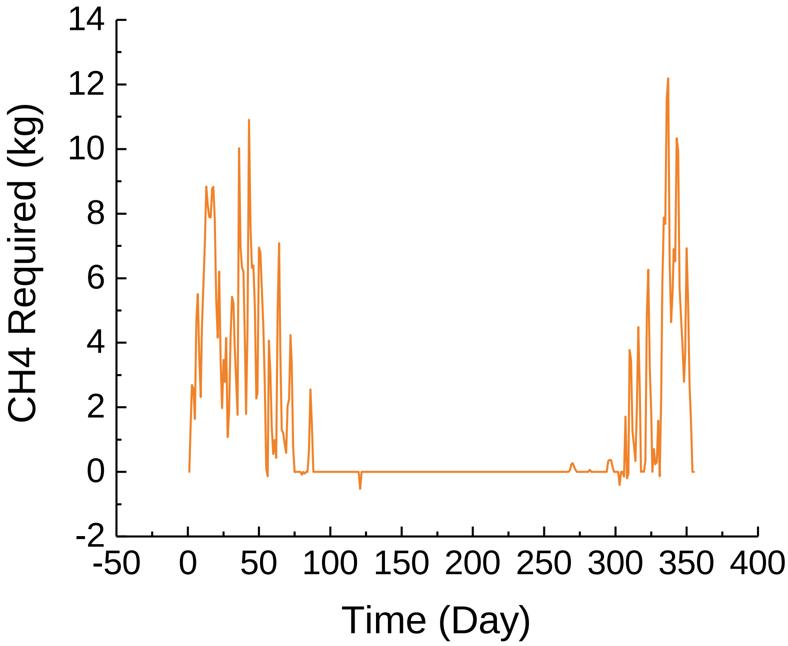

Figure B.8: Daily methane requirements for Grenoble building 15 kWh/m^2.year and STC 6 m^2

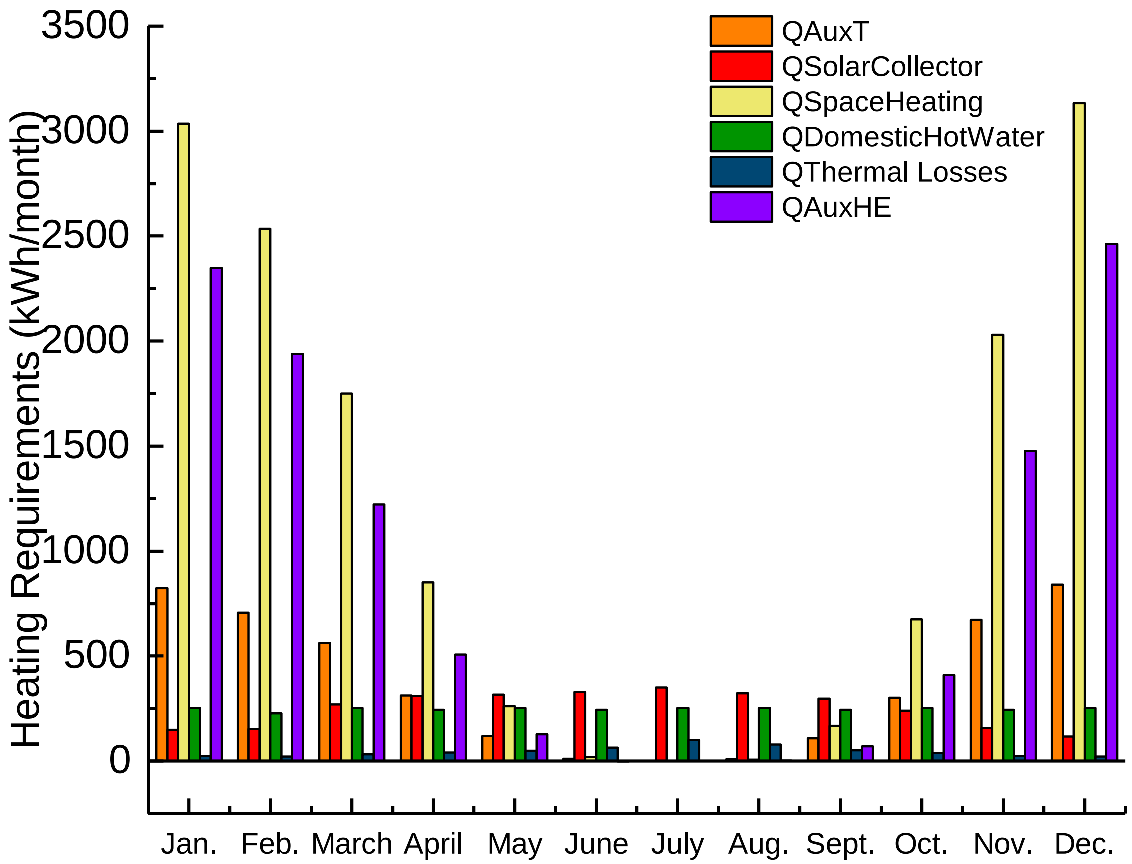

Figure B.9: Monthly heating requirements for Grenoble building 100 kWh/m^2.year and STC 4 m^2

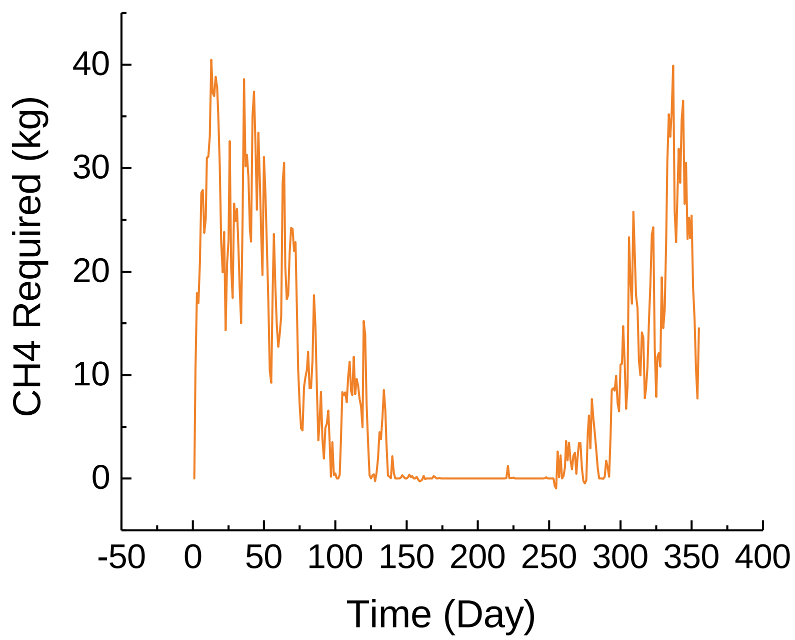

Figure B.10: Daily methane requirements for Grenoble building 100 kWh/m^2.year and STC 4 m^2

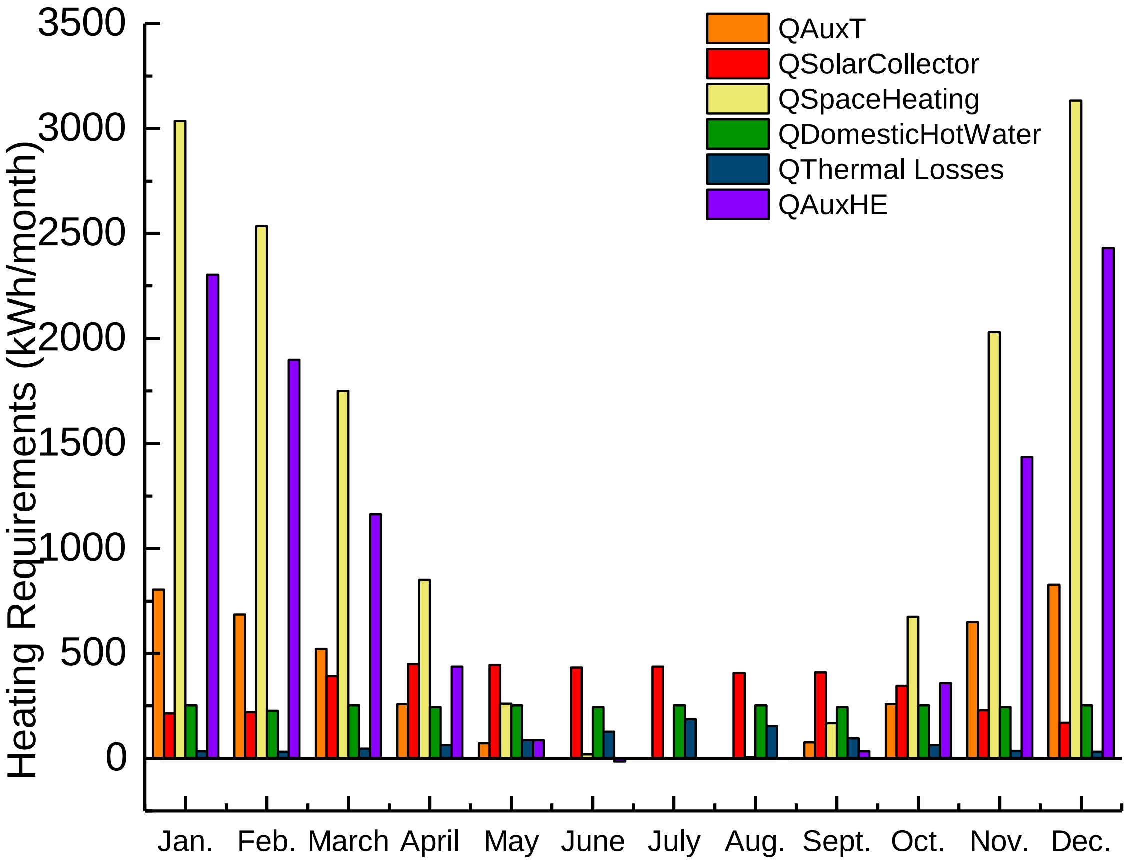

Figure B.11: Monthly heating requirements for Grenoble building 100 kWh/m^2.year and STC 6 m^2

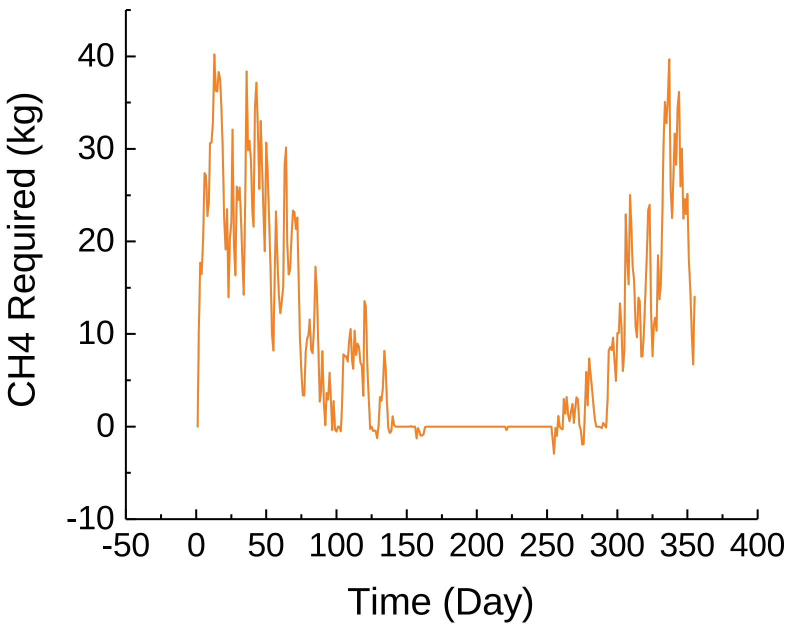

Figure B.12: Daily methane requirements for Grenoble building 100 kWh/m^2.year and STC 6 m^2

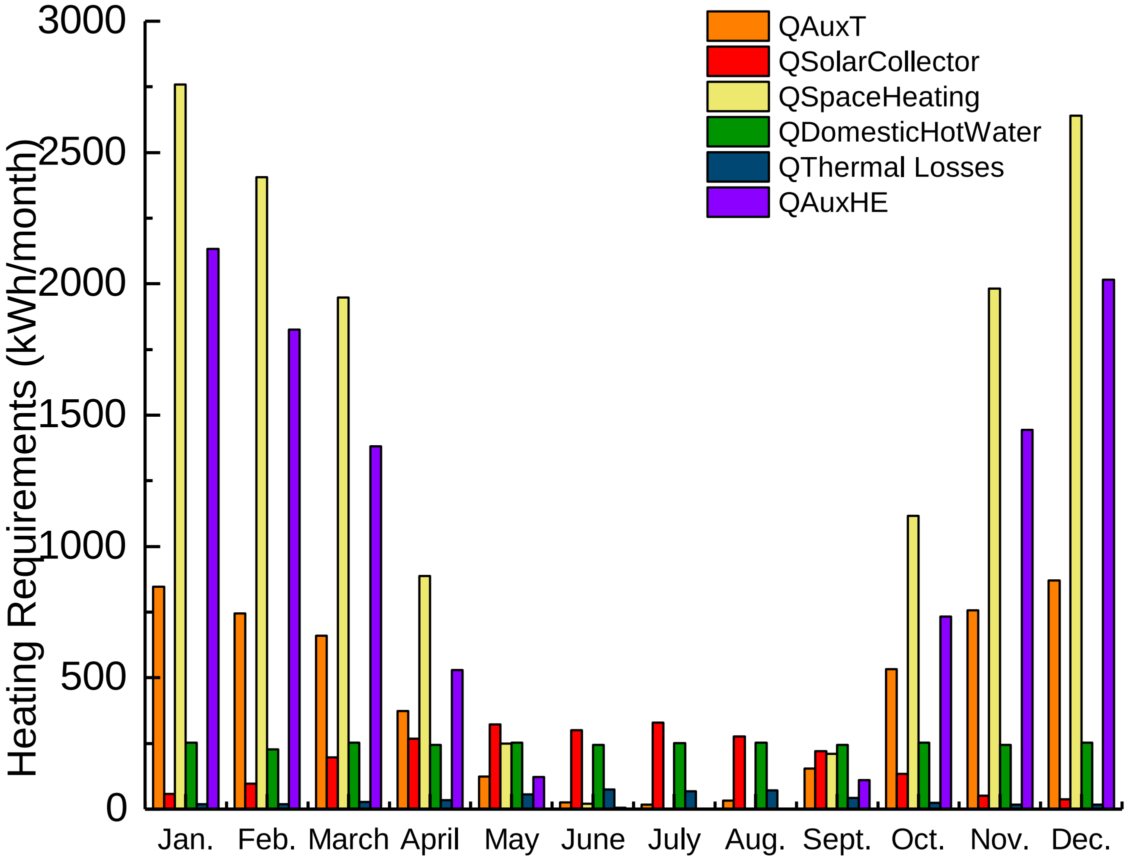

Figure B.13: Monthly heating requirements for Stockholm building 100 kWh/m^2.year and STC 4 m^2

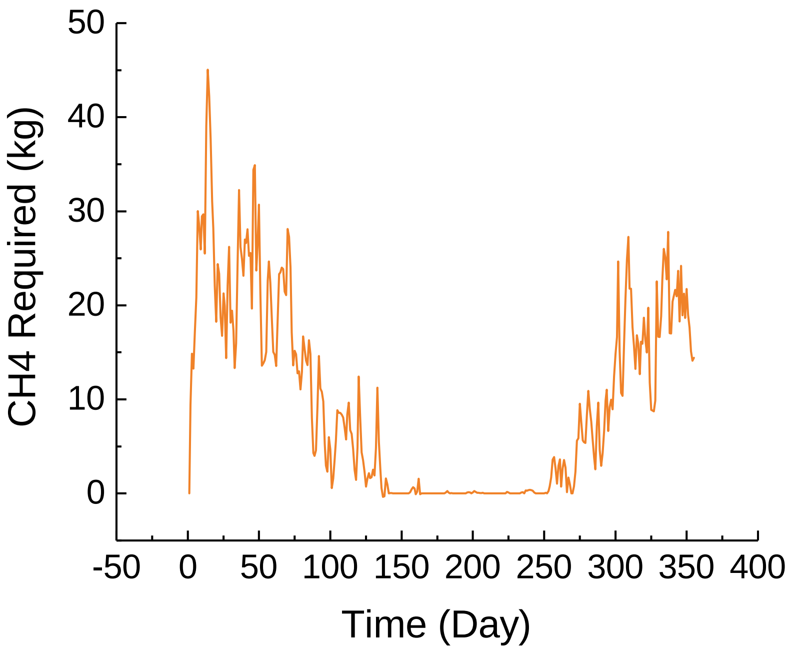

Figure B.14: Daily methane requirements for Stockholm building 100 kWh/m^2.year and STC 4 m^2

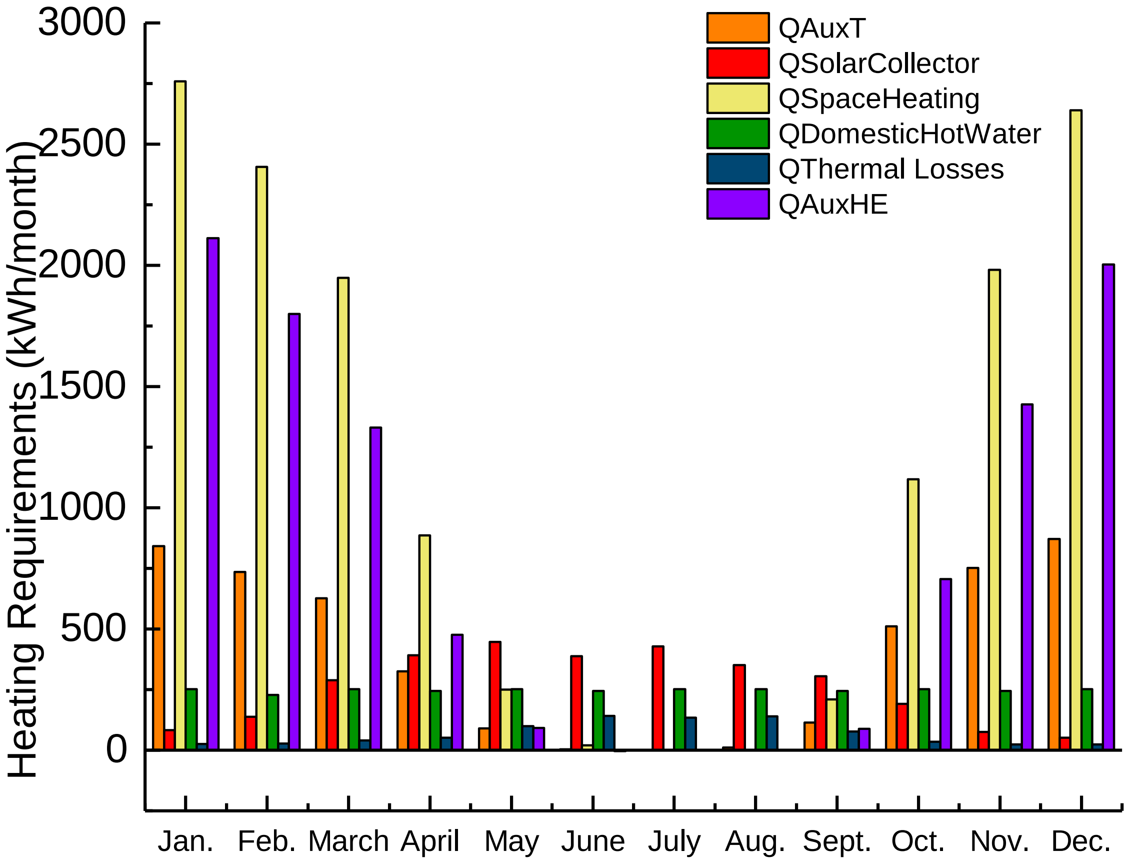

Figure B.15: Monthly heating requirements for Stockholm building 100 kWh/m^2.year and STC 6 m^2

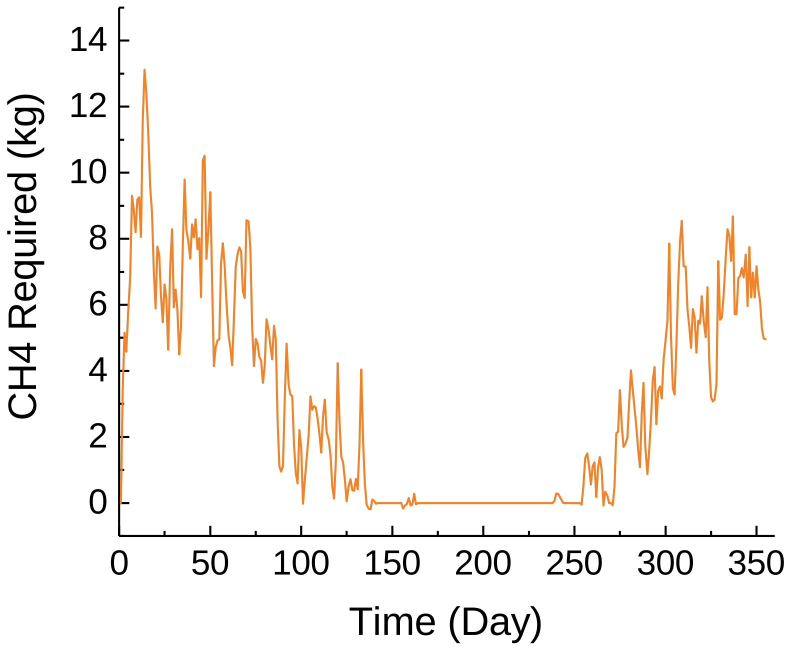

Figure B.16: Daily methane requirements for Stockholm building 100 kWh/m^2.year and STC 6 m^2

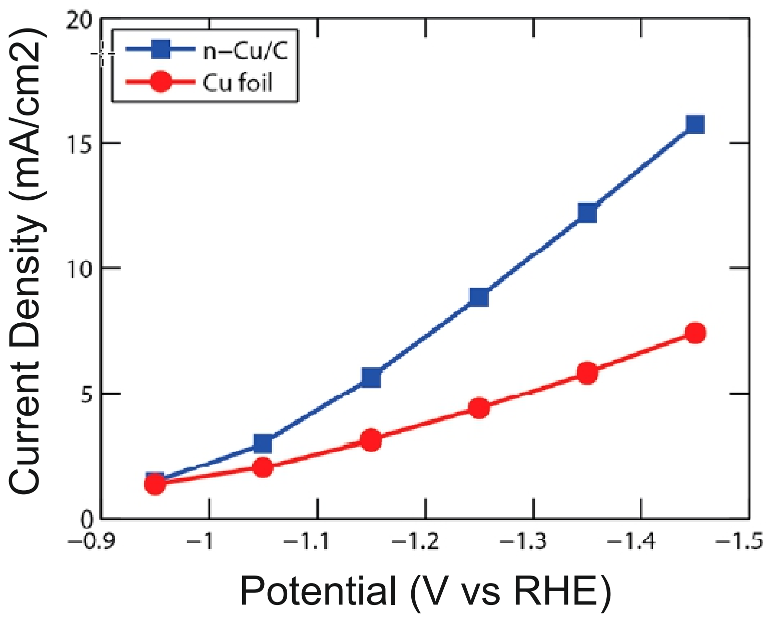

Figure B.17: EC Density current versus V vs RHE results from Manthiram et al work[7]

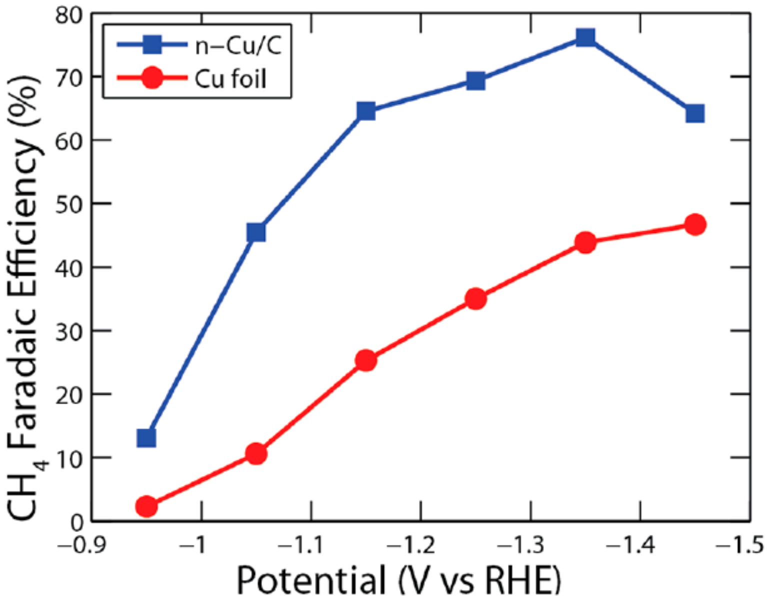

Figure B.18: CH_4 Faradaic efficiency vs V vs RHE results from Manthiram et al work[7]

Annex I

Annex 1 - Code used in MATLAB

In this chapter we can find all the scripts and functions made by the author for this work, for exception the function for curve intersection developed by Douglas M. Shwarz [28].

I.1 Setup Script

Listing I.1: Main setup. Given electrolyzer data, area and PV performance it creates a PV-IV curve and intersects with the electrolyzer IV curve. The results are the methane produced in Liters and the percentage of incidence intersections in the extrapolation curve

```
% clc
% clear all

%% Curvas do electrolyzer
AreaEC = 2500; % Area do electrolyzer cm^2

% Curva EC - mA/cm^2 vs V
ECxx = 1.5 + [0.948162280593782 1.04928608355284 1.14827552251299 ...
    1.24852416237907 1.34808596538736 1.44761453435415];
ECyy = 1e-3 * AreaEC * ([1.52082666601019 2.92373402919672 ...
    5.65452598409690 8.75243100859161 12.1046379951257 15.7110853991778]);
    % Ampere

[ECx,ECy] = extrapolacao(ECxx,ECyy);

% Curva EF do CH4 - % vs V
EFx = 1.5 + [0.950395744128714 1.04722979109900 1.14541326067212 ...
    1.24514726871675 1.34231218372908 1.44488776437005];
EFy = ([12.9739198131569 44.8955495004541 64.6866485013624 ...
    69.0489165693525 75.5443103671986 63.3047878551965]);

% Curva EF do H2 - % vs V
EFH2x = 1.5 + [0.947407494000000 1.04623081700000 1.14895390100000 ...
    1.24836409500000 1.34924146800000 1.45042988400000];
EFH2y = [42.7239649100000 20.3776519300000 13.2389448000000 ...
    12.1127380500000 24.0367968500000 26.0075119600000];

```

```
% Curva Producao Metano - mA/cm^2 vs V
EPCH4xx = 1.5 + [0.949193622991767 1.04995035307903 1.14866446698942 ...
    1.24797557741528 1.34903573961578 1.44922260939283];
EPCH4yy = 1e-3 * AreaEC *([0.245002929476705 1.35652656572821 ...
    3.66335070461624 6.11357735360326 9.26492953837615 10.0577507786241]);
    % Ampere


[EPCH4x,EPCH4y] = extrapolacao(EPCH4xx,EPCH4yy);

% Curva Producao Hidrogenio
EPH2x = EPCH4x;
EPH2y = ECy - EPCH4y;


Dias=[24 48 72 96 120 144 168 192 216 240 264 288 312 336 360 384 408 ...
    432 456 480 504 528 552 576 600 624 648 672 696 720 744 768 792 816 840 ...
    864 888 912 936 960 984 1008 1032 1056 1080 1104 1128 1152 1176 1200 ...
    1224 1248 1272 1296 1320 1344 1368 1392 1416 1440 1464 1488 1512 1536 ...
    1560 1584 1608 1632 1656 1680 1704 1728 1752 1776 1800 1824 1848 1872 ...
    1896 1920 1944 1968 1992 2016 2040 2064 2088 2112 2136 2160 2184 2208 ...
    2232 2256 2280 2304 2328 2352 2376 2400 2424 2448 2472 2496 2520 2544 ...
    2568 2592 2616 2640 2664 2688 2712 2736 2760 2784 2808 2832 2856 2880 ...
    2904 2928 2952 2976 3000 3024 3048 3072 3096 3120 3144 3168 3192 3216 ...
    3240 3264 3288 3312 3336 3360 3384 3408 3432 3456 3480 3504 3528 3552 ...
    3576 3600 3624 3648 3672 3696 3720 3744 3768 3792 3816 3840 3864 3888 ...
    3912 3936 3960 3984 4008 4032 4056 4080 4104 4128 4152 4176 4200 4224 ...
    4248 4272 4296 4320 4344 4368 4392 4416 4440 4464 4488 4512 4536 4560 ...
    4584 4608 4632 4656 4680 4704 4728 4752 4776 4800 4824 4848 4872 4896 ...
    4920 4944 4968 4992 5016 5040 5064 5088 5112 5136 5160 5184 5208 5232 ...
    5256 5280 5304 5328 5352 5376 5400 5424 5448 5472 5496 5520 5544 5568 ...
    5592 5616 5640 5664 5688 5712 5736 5760 5784 5808 5832 5856 5880 5904 ...
    5928 5952 5976 6000 6024 6048 6072 6096 6120 6144 6168 6192 6216 6240 ...
    6264 6288 6312 6336 6360 6384 6408 6432 6456 6480 6504 6528 6552 6576 ...
    6600 6624 6648 6672 6696 6720 6744 6768 6792 6816 6840 6864 6888 6912 ...
    6936 6960 6984 7008 7032 7056 7080 7104 7128 7152 7176 7200 7224 7248 ...
    7272 7296 7320 7344 7368 7392 7416 7440 7464 7488 7512 7536 7560 7584 ...
    7608 7632 7656 7680 7704 7728 7752 7776 7800 7824 7848 7872 7896 7920 ...
    7944 7968 7992 8016 8040 8064 8088 8112 8136 8160 8184 8208 8232 8256 ...
    8280 8304 8328 8352 8376 8400 8424 8448 8472 8496 8520 8544 8568 8592 ...
    8616 8640 8664 8688 8712 8736 8760 8784];

%% Avaliar se e necessario ver as curvas IV
 answer = questdlg(['Would you like to see IV curves interception' ...
     'with Eletrolyzer Curves?'], 'Interative plot', 'Yes','No','No');
 % Resposta
 switch answer
     case 'Yes'
         VerPlot = 1;
     case 'No'
         VerPlot = 0;
 end

% Ler ficheiro dados vindo do TRNSYS
 [MatrizTotal,Success,Caso] = get_files();
```

```
 if Success == 0
     return
 end

% Ler Dados do ficheiro e guardar em variaveis locais
Tempo = MatrizTotal(2:end,1);
Isaturacao = MatrizTotal(2:end,2);
Iphoto = MatrizTotal(2:end,3);
Tcurrent = MatrizTotal(2:end,4);
Vopencircuit = MatrizTotal(2:end,5);
Ishortcircuit = MatrizTotal(2:end,6);
DiodeFactor = MatrizTotal(2:end,7);
CellsSeries = MatrizTotal(2:end,8);
ModulosSeries = MatrizTotal(2:end,9);
ModulosParalelo = MatrizTotal(2:end,10);
FFvalue = MatrizTotal(2:end,11);
Rseries = MatrizTotal(2:end,12);


% Constantes
Rp = 1e6;% resistencia paralelo (shunt) (ohm)
q = 1.6e-19; % carga electrao(C)
k = 1.38e-23; % boltzman
F = 96485; % Coulomb
dt = (Tempo(2) - Tempo(1)) * 3600; % segundos
R = 0.082; % atm/mole K
Pressao = 1; % atm
Tamb = 298; % K
DensidadeCH4 = 0.668;
Voc= 0; % Voc inicial
i = 0;  % Set initial current i=0
idx=0; % Contador
Metano = 0; % Somatorio do volume de metano
Hidrogenio = 0;
Oxigenio = 0;
MO2 = 15.999; %
Omega = 0;
b=1;
VolumeCH4Dia=0;
ProdMetanoDia=0;

% Constantes do Trnsys
A = DiodeFactor(1); % Factor do diodo, TRNSYS
Ns = CellsSeries(1); % Numero celulas em serie, TRNSYS
Nms = ModulosSeries(1); % Numero de modulos em serie, TRNSYS
Nmp = ModulosParalelo(1); % Numero de modulos em paralelo, TRNSYS

%% Vectores zeros
Vop = zeros(1,length(Tempo));
Iop = zeros(1,length(Tempo));
VolumeCH4 = zeros(1,length(Tempo));
VolumeH2 = zeros(1,length(Tempo));
VolumeO2 = zeros(1,length(Tempo));
etaCH4 = zeros(1,length(Tempo));
etaH2 = zeros(1,length(Tempo));
```

```
Total=1:length(Tempo);

for a=Total
    % Cada hora que passa tem se uma nova curva IV e uma nova intersecao
    if a == 0
        continue
    end
    Producao = 1;
    %% Leitura de Constantes do TRNSYS
    Isat = Isaturacao(a);        % Corrente saturacao (A) I0
    Iph = Iphoto(a);             % Photocorrente (A) IL
    TK = Tcurrent(a);            % Temperatura de juncao (K)
    Voc = Vopencircuit(a);       % TRNSYS Voltagem circuito aberto (V)
    Rs = Rseries(a);             % Resistencia series (ohm)

    %% Calculo curva IV
    [V,I,P] = CalcIV(Voc,Iph,Isat,TK,Ns,Nms,Nmp,Rs,Rp,A);

    %% Calculo da Intersecao
    if Voc == 0
       Resx=0;
       Resy=0;
       Producao = 0;
    else
        [Resx,Resy] = intersections(ECx,ECy,V,I);
        if isempty(Resx)
            Resx = 0;
            Resy = 0;
        end
    end
    Vop(a) = Resx;
    Iop(a) = Resy;

    %% Calculo de Eficiencia Faradaica
    if Vop(a) == 0 % Nao houve intersecao, logo nao ha producao
       etaCH4(a) = 0;
       etaH2(a) = 0;
    elseif Vop(a) >= EFx(end)
    % Vop e superior aos valores experimentais da eficiencia faradaica
    % Neste caso a intersecao da-se na curva EXTRAPOLADA,
    % Caso 1: considera-se eta 0.6 e 0.2 para CH4 e H2
    % Caso 2: considera-se eta 0.4 e 0.05 para CH4 e H2
            etaCH4(a) = 0.4;
            etaH2(a) = 0.05;
            Omega = Omega + 1;
            % Contador de intersecoes na curva extrapolada
    else
    % Caso nao seja, o eta e dado pelo grafico de Eficiencias faradaicas
    % Interseta a interpolacao do valor Tensao de Operacao no
    % grafico % vs V da curva Eficiencia Faradaica
       etaCH4(a) = spline(EFx,EFy,Vop(a)) / 100;
       etaH2(a) = spline(EFH2x,EFH2y,Vop(a)) / 100;
    end

    %% Conversao para H2
```

```
    Farad = Iop(a) * dt * 1/F;
    moleH2 = Farad * 1/2;
    VolumeH2(a) = (moleH2 * R * Tamb)/Pressao * etaH2(a); % PV = nRT <=>
    % <=> V = (nRT)/P
    Hidrogenio = Hidrogenio + VolumeH2(a); % Somatorio, Litros

    %% Conversao para Metano
    Farad = Iop(a) * dt * 1/F;
    moleCH4 = Farad * 1/8;
    VolumeCH4(a) = (moleCH4 * R * Tamb)/Pressao * etaCH4(a); % PV = nRT <=>
    % <=> V = (nRT)/P
    Metano = Metano + VolumeCH4(a); % Somatorio, Litros

    %% Conversao para O2
    if Producao == 1
        VolumeO2(a) = 24.4 * (2*moleCH4 + moleH2/2) ; % VM = V / n ;
        % devido a anodic half reaction do CO2 + 2H2O -> Ch4 + 2O2
        % e da electrolise da agua
        Oxigenio = Oxigenio + VolumeO2(a); % Somatorio, Litros
    end

    if VerPlot == 1
         figure(1)
         hold off

         out=sprintf(['T = %d | eta = %0.2f | Vop = %0.3f V' ...
          '| Iop = %0.3f A | FF = %0.2f | Iprod = %0.2f A' ...
          '| VolumCH4 = %0.3f | CH4Total = %0.2d'],a,etaCH4(a)', ...
          Vop(a),Iop(a),FFvalue(a),IprodCH4(a),VolumeCH4(a),Metano);
         plot(ECx,ECy,'b',ECxx,ECyy,'r')  % Grafico EC
         hold on
         title(out)
         ylabel('Corrente (A)')
         xlabel('Tensao (V)')
         plot(V,I)
         plot(Vop(a),Iop(a),'og'); %Grafico intersecao

    end

    % Guarda os valores em dias
    VolumeCH4Dia = VolumeCH4Dia + VolumeCH4(a); %% Guarda a producao
    % a cada hora
    if Tempo(a)==Dias(b)  % Tempo em horas. Dias em Horas
        ProdMetanoDia(b)=VolumeCH4Dia;
        VolumeCH4Dia=0;
        b=b+1;
    end

end

% Plots graficos
    figure(2)
    hold off
    xlabel('Tempo (h)')
    ylabel('Eficiencia Faradaica (%)')
```

```
    hold on
    plot(Tempo,100*etaCH4,'b');

    figure(3)
    hold off
    xlabel('Tempo (h)')
    ylabel('Volume producao CH4 (L)')
    hold on
    plot(Tempo,VolumeCH4,'m');

    figure(4)
    hold off
    xlabel('Tempo (h)')
    ylabel('Volume producao H2 (L)')
    hold on
    plot(Tempo,VolumeH2,'m');

    figure(5)
    hold off
    xlabel('Tempo (h)')
    ylabel('Corrente Producao Metano (A)')
    hold on
    plot(Tempo,IprodCH4,'k');

    figure(5)
    hold off
    xlabel('Tempo (h)')
    ylabel('Producao Metano por dia (L)')
    hold on
    plot(ProdMetanoDia,'k');

    Beta= Omega/length(Tempo) * 100; % Percentagem de incidencias na
    % curva extrapolada

   sprintf(['%s, Producao de metano: %0.2f L, Hidrogenio: %0.2f L e '...
       'Oxigenio: %0.2f L durante %d horas. Com %d interseccoes na curva'...
       'extrapolada, %0.2f%% incidencias.'],Caso,Metano,Hidrogenio,...
        Oxigenio,length(Total),Omega,Beta)
  end
```

I.2 Function to Calculate IV curve

```
function [outputArg1,outputArg2,outputArg3] = CalcIV(Voc,IL,I0,TK,Ns,...
    Nms,Nmp,Rs,Rsh,A)
% Given Voc_T,IL,I0,TK,Ns,Nms,Nmp,Rs,Rsh,A, IV curve is calculated.
% Outputs are 3 vectors:
% [outputArg1,outputArg2,outputArg3]
% Voltages, Current and Power
%
% Voc - Open circuit current (V)
% IL - Photo current diode (A)
% I0 - Reverse saturation current (A)
```

```
% TK - Ambient temperature (Kelvin)
% Ns - Nnumber cells in series
% Nms - Number of modules in series
% Nmp - Number of modules in parallels
% Rs - Series resistance (Ohm)
% Rsh - Shunt Resistance
% A - Quality factor

q = 1.6e-19; % electro charge (C)
k = 1.38e-23; % boltzman constant

vt=(A*k*TK*Ns)/q;

i = 0; % Set initial current i=0
idx=1;
I = zeros(1, length(0:Voc/150:Voc));
for V=0:Voc/150:Voc
    I(idx)= IL - I0*(exp((V+(i*Rs))/vt)-1)-((V+(i*Rs))/Rsh);
    i = I(idx); %Update Current value
    idx=idx+1;
end
V=0:Voc/150:Voc;
% This curve is for 1 cell
% We need to multiply V by number of cells in series and
% I by number of modules in parallel

V = V.*Nms.*Ns;
I = I.*Nmp;
P = I.*V;

outputArg1=V;
outputArg2=I;
outputArg3=P;

end
```

I.3 Extrapolate function

```
function [ECx,ECy] = extrapolacao(ValorX,ValorY)

global x y

% enter data and plot it
x = ValorX;
y = ValorY;


c0 = [1 1];
fx = 'OF_exp_regr';
options = optimset('MaxFunEvals',1000);
[c, f, EF, out] = fminsearch(fx, c0,options);
yf = c(1) * exp(c(2) * x);
```

```
x2 = linspace(x(end)+0.01,4,20); % vai ate 4V
y2 = c(1) * exp(c(2) * x2);

%% plot results after optimization
% figure
% plot(x, y, 'g-o', x, yf, 'bo')
% legend('measured data', 'final fit')
% hold on
% plot(x2,y2,'r')

%% Outputs
ECx = horzcat(x,x2);
ECy = horzcat(y,y2);
```

I.4 Extrapolate equation

```
function U = OF_exp_regr(c)
global x y

% try coefficients
y2 = c(1) * exp(c(2) * x);

% try to match original data, and return difference
U = norm(y2 - y, 1);
```

I.5 Function to fetch files

```
function [MatrizTotal,Success,baseFileName] = get_files()

[file,path] = uigetfile('.txt');
[folder, baseFileName, extension] = fileparts(file);

MatrizTotal = dlmread(fullfile(path,file),'',2,0);
Success = 1;
end
```

I.6 Funtion to calculate intersection of two pairs of vectors

Listing I.6: Function created by Douglas M. Schwarz [28]

```
function [x0,y0,iout,jout] = intersections(x1,y1,x2,y2,robust)
%INTERSECTIONS Intersections of curves.
%   Computes the (x,y) locations where two curves intersect.  The curves
%   can be broken with NaNs or have vertical segments.
%
% Example:
```

```
%   [X0,Y0] = intersections(X1,Y1,X2,Y2,ROBUST);
%
% where X1 and Y1 are equal-length vectors of at least two points and
% represent curve 1.  Similarly, X2 and Y2 represent curve 2.
% X0 and Y0 are column vectors containing the points at which the two
% curves intersect.
%
% ROBUST (optional) set to 1 or true means to use a slight variation of the
% algorithm that might return duplicates of some intersection points, and
% then remove those duplicates.  The default is true, but since the
% algorithm is slightly slower you can set it to false if you know that
% your curves don't intersect at any segment boundaries.  Also, the robust
% version properly handles parallel and overlapping segments.
%
% The algorithm can return two additional vectors that indicate which
% segment pairs contain intersections and where they are:
%
%   [X0,Y0,I,J] = intersections(X1,Y1,X2,Y2,ROBUST);
%
% For each element of the vector I, I(k) = (segment number of (X1,Y1)) +
% (how far along this segment the intersection is).  For example, if I(k) =
% 45.25 then the intersection lies a quarter of the way between the line
% segment connecting (X1(45),Y1(45)) and (X1(46),Y1(46)).  Similarly for
% the vector J and the segments in (X2,Y2).
%
% You can also get intersections of a curve with itself.  Simply pass in
% only one curve, i.e.,
%
%   [X0,Y0] = intersections(X1,Y1,ROBUST);
%
% where, as before, ROBUST is optional.

% Version: 2.0, 25 May 2017
% Author:  Douglas M. Schwarz
% Email:   dmschwarz=ieee*org, dmschwarz=urgrad*rochester*edu
% Real_email = regexprep(Email,{'=','*'},{'@','.'})


% Theory of operation:
%
% Given two line segments, L1 and L2,
%
%   L1 endpoints:  (x1(1),y1(1)) and (x1(2),y1(2))
%   L2 endpoints:  (x2(1),y2(1)) and (x2(2),y2(2))
%
% we can write four equations with four unknowns and then solve them.  The
% four unknowns are t1, t2, x0 and y0, where (x0,y0) is the intersection of
% L1 and L2, t1 is the distance from the starting point of L1 to the
% intersection relative to the length of L1 and t2 is the distance from the
% starting point of L2 to the intersection relative to the length of L2.
%
% So, the four equations are
%
%    (x1(2) - x1(1))*t1 = x0 - x1(1)
%    (x2(2) - x2(1))*t2 = x0 - x2(1)
```

```
%    (y1(2) - y1(1))*t1 = y0 - y1(1)
%    (y2(2) - y2(1))*t2 = y0 - y2(1)
%
% Rearranging and writing in matrix form,
%
%  [x1(2)-x1(1)       0       -1   0;      [t1;      [-x1(1);
%        0       x2(2)-x2(1)  -1   0;   *   t2;   =   -x2(1);
%   y1(2)-y1(1)       0        0  -1;       x0;       -y1(1);
%        0       y2(2)-y2(1)   0  -1]       y0]       -y2(1)]
%
% Let's call that A*T = B.  We can solve for T with T = A\B.
%
% Once we have our solution we just have to look at t1 and t2 to determine
% whether L1 and L2 intersect.  If 0 <= t1 < 1 and 0 <= t2 < 1 then the two
% line segments cross and we can include (x0,y0) in the output.
%
% In principle, we have to perform this computation on every pair of line
% segments in the input data.  This can be quite a large number of pairs so
% we will reduce it by doing a simple preliminary check to eliminate line
% segment pairs that could not possibly cross.  The check is to look at the
% smallest enclosing rectangles (with sides parallel to the axes) for each
% line segment pair and see if they overlap.  If they do then we have to
% compute t1 and t2 (via the A\B computation) to see if the line segments
% cross, but if they don't then the line segments cannot cross.  In a
% typical application, this technique will eliminate most of the potential
% line segment pairs.


% Input checks.
if verLessThan('matlab','7.13')
    error(nargchk(2,5,nargin)) %#ok<NCHKN>
else
    narginchk(2,5)
end

% Adjustments based on number of arguments.
switch nargin
    case 2
        robust = true;
        x2 = x1;
        y2 = y1;
        self_intersect = true;
    case 3
        robust = x2;
        x2 = x1;
        y2 = y1;
        self_intersect = true;
    case 4
        robust = true;
        self_intersect = false;
    case 5
        self_intersect = false;
end

% x1 and y1 must be vectors with same number of points (at least 2).
```

```
if sum(size(x1) > 1) ~= 1 || sum(size(y1) > 1) ~= 1 || ...
        length(x1) ~= length(y1)
    error('X1 and Y1 must be equal-length vectors of at least 2 points.')
end
% x2 and y2 must be vectors with same number of points (at least 2).
if sum(size(x2) > 1) ~= 1 || sum(size(y2) > 1) ~= 1 || ...
        length(x2) ~= length(y2)
    error('X2 and Y2 must be equal-length vectors of at least 2 points.')
end


% Force all inputs to be column vectors.
x1 = x1(:);
y1 = y1(:);
x2 = x2(:);
y2 = y2(:);

% Compute number of line segments in each curve and some differences we'll
% need later.
n1 = length(x1) - 1;
n2 = length(x2) - 1;
xy1 = [x1 y1];
xy2 = [x2 y2];
dxy1 = diff(xy1);
dxy2 = diff(xy2);


% Determine the combinations of i and j where the rectangle enclosing the
% i'th line segment of curve 1 overlaps with the rectangle enclosing the
% j'th line segment of curve 2.

% Original method that works in old MATLAB versions, but is slower than
% using binary singleton expansion (explicit or implicit).
% [i,j] = find( ...
%   repmat(mvmin(x1),1,n2) <= repmat(mvmax(x2).',n1,1) & ...
%   repmat(mvmax(x1),1,n2) >= repmat(mvmin(x2).',n1,1) & ...
%   repmat(mvmin(y1),1,n2) <= repmat(mvmax(y2).',n1,1) & ...
%   repmat(mvmax(y1),1,n2) >= repmat(mvmin(y2).',n1,1));

% Select an algorithm based on MATLAB version and number of line
% segments in each curve.  We want to avoid forming large matrices for
% large numbers of line segments.  If the matrices are not too large,
% choose the best method available for the MATLAB version.
if n1 > 1000 || n2 > 1000 || verLessThan('matlab','7.4')
    % Determine which curve has the most line segments.
    if n1 >= n2
        % Curve 1 has more segments, loop over segments of curve 2.
        ijc = cell(1,n2);
        min_x1 = mvmin(x1);
        max_x1 = mvmax(x1);
        min_y1 = mvmin(y1);
        max_y1 = mvmax(y1);
        for k = 1:n2
            k1 = k + 1;
            ijc{k} = find( ...
```

```
                min_x1 <= max(x2(k),x2(k1)) & max_x1 >= min(x2(k),x2(k1)) & ...
                min_y1 <= max(y2(k),y2(k1)) & max_y1 >= min(y2(k),y2(k1)));
            ijc{k}(:,2) = k;
        end
        ij = vertcat(ijc{:});
        i = ij(:,1);
        j = ij(:,2);
    else
        % Curve 2 has more segments, loop over segments of curve 1.
        ijc = cell(1,n1);
        min_x2 = mvmin(x2);
        max_x2 = mvmax(x2);
        min_y2 = mvmin(y2);
        max_y2 = mvmax(y2);
        for k = 1:n1
            k1 = k + 1;
            ijc{k}(:,2) = find( ...
                min_x2 <= max(x1(k),x1(k1)) & max_x2 >= min(x1(k),x1(k1)) & ...
                min_y2 <= max(y1(k),y1(k1)) & max_y2 >= min(y1(k),y1(k1)));
            ijc{k}(:,1) = k;
        end
        ij = vertcat(ijc{:});
        i = ij(:,1);
        j = ij(:,2);
    end

elseif verLessThan('matlab','9.1')
    % Use bsxfun.
    [i,j] = find( ...
        bsxfun(@le,mvmin(x1),mvmax(x2).') & ...
        bsxfun(@ge,mvmax(x1),mvmin(x2).') & ...
        bsxfun(@le,mvmin(y1),mvmax(y2).') & ...
        bsxfun(@ge,mvmax(y1),mvmin(y2).'));

else
    % Use implicit expansion.
    [i,j] = find( ...
        mvmin(x1) <= mvmax(x2).' & mvmax(x1) >= mvmin(x2).' & ...
        mvmin(y1) <= mvmax(y2).' & mvmax(y1) >= mvmin(y2).');

end


% Find segments pairs which have at least one vertex = NaN and remove them.
% This line is a fast way of finding such segment pairs.  We take
% advantage of the fact that NaNs propagate through calculations, in
% particular subtraction (in the calculation of dxy1 and dxy2, which we
% need anyway) and addition.
% At the same time we can remove redundant combinations of i and j in the
% case of finding intersections of a line with itself.
if self_intersect
    remove = isnan(sum(dxy1(i,:) + dxy2(j,:),2)) | j <= i + 1;
else
    remove = isnan(sum(dxy1(i,:) + dxy2(j,:),2));
end
```

```
i(remove) = [];
j(remove) = [];

% Initialize matrices.  We'll put the T's and B's in matrices and use them
% one column at a time.  AA is a 3-D extension of A where we'll use one
% plane at a time.
n = length(i);
T = zeros(4,n);
AA = zeros(4,4,n);
AA([1 2],3,:) = -1;
AA([3 4],4,:) = -1;
AA([1 3],1,:) = dxy1(i,:).';
AA([2 4],2,:) = dxy2(j,:).';
B = -[x1(i) x2(j) y1(i) y2(j)].';

% Loop through possibilities.  Trap singularity warning and then use
% lastwarn to see if that plane of AA is near singular.  Process any such
% segment pairs to determine if they are colinear (overlap) or merely
% parallel.  That test consists of checking to see if one of the endpoints
% of the curve 2 segment lies on the curve 1 segment.  This is done by
% checking the cross product
%
%   (x1(2),y1(2)) - (x1(1),y1(1)) x (x2(2),y2(2)) - (x1(1),y1(1)).
%
% If this is close to zero then the segments overlap.

% If the robust option is false then we assume no two segment pairs are
% parallel and just go ahead and do the computation.  If A is ever singular
% a warning will appear.  This is faster and obviously you should use it
% only when you know you will never have overlapping or parallel segment
% pairs.

if robust
    overlap = false(n,1);
    warning_state = warning('off','MATLAB:singularMatrix');
    % Use try-catch to guarantee original warning state is restored.
    try
        lastwarn('')
        for k = 1:n
            T(:,k) = AA(:,:,k)\B(:,k);
            [unused,last_warn] = lastwarn; %#ok<ASGLU>
            lastwarn('')
            if strcmp(last_warn,'MATLAB:singularMatrix')
                % Force in_range(k) to be false.
                T(1,k) = NaN;
                % Determine if these segments overlap or are just parallel.
                overlap(k) = rcond([dxy1(i(k),:);xy2(j(k),:) - ...
                    xy1(i(k),:)]) < eps;
            end
        end
        warning(warning_state)
    catch err
        warning(warning_state)
        rethrow(err)
    end
```

```
    % Find where t1 and t2 are between 0 and 1 and return the corresponding
    % x0 and y0 values.
    in_range = (T(1,:) >= 0 & T(2,:) >= 0 & T(1,:) <= 1 & T(2,:) <= 1).';
    % For overlapping segment pairs the algorithm will return an
    % intersection point that is at the center of the overlapping region.
    if any(overlap)
        ia = i(overlap);
        ja = j(overlap);
        % set x0 and y0 to middle of overlapping region.
        T(3,overlap) = (max(min(x1(ia),x1(ia+1)),min(x2(ja),x2(ja+1))) + ...
            min(max(x1(ia),x1(ia+1)),max(x2(ja),x2(ja+1)))).'/2;
        T(4,overlap) = (max(min(y1(ia),y1(ia+1)),min(y2(ja),y2(ja+1))) + ...
            min(max(y1(ia),y1(ia+1)),max(y2(ja),y2(ja+1)))).'/2;
        selected = in_range | overlap;
    else
        selected = in_range;
    end
    xy0 = T(3:4,selected).';

    % Remove duplicate intersection points.
    [xy0,index] = unique(xy0,'rows');
    x0 = xy0(:,1);
    y0 = xy0(:,2);

    % Compute how far along each line segment the intersections are.
    if nargout > 2
        sel_index = find(selected);
        sel = sel_index(index);
        iout = i(sel) + T(1,sel).';
        jout = j(sel) + T(2,sel).';
    end
else % non-robust option
    for k = 1:n
        [L,U] = lu(AA(:,:,k));
        T(:,k) = U\(L\B(:,k));
    end

    % Find where t1 and t2 are between 0 and 1 and return the corresponding
    % x0 and y0 values.
    in_range = (T(1,:) >= 0 & T(2,:) >= 0 & T(1,:) < 1 & T(2,:) < 1).';
    x0 = T(3,in_range).';
    y0 = T(4,in_range).';

    % Compute how far along each line segment the intersections are.
    if nargout > 2
        iout = i(in_range) + T(1,in_range).';
        jout = j(in_range) + T(2,in_range).';
    end
end

% Plot the results (useful for debugging).
% plot(x1,y1,x2,y2,x0,y0,'ok');

function y = mvmin(x)
% Faster implementation of movmin(x,k) when k = 1.
```

```
y = min(x(1:end-1),x(2:end));

function y = mvmax(x)
% Faster implementation of movmax(x,k) when k = 1.
y = max(x(1:end-1),x(2:end));
```